

# Towards large-scale, automated, accurate detection of CCTV camera objects using computer vision

Applications and implications for privacy, anonymity, surveillance, safety, and cybersecurity

(Preprint)

Hannu Turtiainen<sup>¶ †</sup>, Andrei Costin<sup>¶ ⊗</sup>, Tuomo Lahtinen<sup>§</sup>,  
Lauri Sintonen<sup>§</sup>, and Timo Hämäläinen<sup>¶</sup>

*University of Jyväskylä*

Jyväskylä, Finland

<sup>¶</sup>{turthzu,ancostin,timoh}@jyu.fi,

<sup>§</sup>{tuomo.t.lahtinen,lauri.m.j.sintonen}@student.jyu.fi

**Abstract**—While the earliest known CCTV camera was developed almost a century ago back in 1927, currently, it is assumed as granted there are about 770 millions CCTV cameras around the globe, and their number is casually predicted to surpass 1 billion in 2021. Similarly to the first prototypes from 1927, at present the main promoted benefits for using and deploying CCTV cameras are physical security, safety, and prophylactics of crime. At the same time the increasing, widespread, unwarranted, and unaccountable use of CCTV cameras globally raises privacy risks and concerns for the last several decades. Recent technological advances implemented in CCTV cameras such as AI-based facial recognition and IoT connectivity only fuel further concerns raised by privacy advocates.

In order to withstand the ever-increasing invasion of privacy by CCTV cameras and technologies, on par *CCTV-aware solutions* must exist that provide privacy, safety, and cybersecurity features. We argue that a first important step towards such CCTV-aware solutions must be a mapping system (e.g., Google Maps, OpenStreetMap) that provides both privacy and safety routing and navigation options. However, this in turn requires that the mapping system contains updated information on CCTV cameras' exact geo-location, coverage area, and possibly other meta-data (e.g., resolution, facial recognition features, operator). Such information is however missing from current mapping systems, and there are several ways to fix this. One solution is to perform CCTV camera detection on geo-location tagged images, e.g., street view imagery on various platforms, user images publicly posted in image sharing platforms such as Flickr. Additionally, mobile devices, equipped with video input and GPS, can be designed and built that can aid real-time data collection and mapping of CCTV cameras in the real-world. At present, the only fast, scalable and feasible way to achieve these is to apply computer vision object detection techniques. Unfortunately, to the best of our knowledge, there are no computer vision models for CCTV camera object detection as well as no mapping system that supports privacy and safety routing options.

To close these gaps, with this paper we introduce the first and only computer vision MS COCO-compatible models that are able to accurately detect CCTV and video surveillance cameras in images and video frames. To this end, our best detectors were built using 8387 images that were manually reviewed

and annotated to contain 10419 CCTV camera instances, and achieve an accuracy of up to 98,7%. Moreover, we build and evaluate multiple models, present a comprehensive comparison of their performance, and outline core challenges associated with such research. We also present possible privacy-, safety-, and security-related practical applications of our core work, including *previews and excerpts* from our working prototypes of CCTV-aware privacy and safety routing and navigation. Last but not least, we release as open-data and open-source relevant data and code that can be used to validate and further extend our work.

*a) Keywords:* : Privacy-enhancing technologies and anonymity; Usable security and privacy; Research on surveillance and censorship; Privacy; Anonymity;

## I. INTRODUCTION

CCTV and video surveillance cameras represent nowadays some of the most ubiquitous technology, and it is almost impossible to live a day without getting into the field of view of at least one, if not dozens of, CCTV camera(s) [2, 3]. At present, CCTV cameras are an integral part of any infrastructure (e.g., cities, buildings, streets, businesses), and it is expected that by 2021 there will be more than 1 billion CCTV cameras globally [4]. Meanwhile, the earliest known precursor of a modern CCTV camera goes back as early as 1927 when the Soviet inventor Leon Theremin installed the first real-world usable prototypes of then-called *distance vision* along the Kremlin premises [5]. It was a mechanically-operated device that transmitted a few hundred image-lines which allowed its operators to distinguish and even recognize faces.

In terms of cybersecurity, CCTV cameras, DVRs, and video surveillance systems are already known to be the subject of numerous cyberattacks [6], and they were also the main culprit behind the now legendary and massive attack by the Mirai IoT botnet [7]. At the same time, it is long and well known that CCTV cameras raise concerns and pose risks related to privacy [8, 9, 10, 11, 12]. However, it is very hard (if not impossible) at present to accurately and objectively assess and address the privacy risks and implications.

<sup>†</sup> This paper is based on author's MSc thesis [1].

<sup>⊗</sup> Corresponding and original idea's author.

There are several ways to mitigate the privacy risks posed by CCTV cameras (including their additional features such as face recognition). One possible and commonly used and promoted method is to use artistic (but perhaps unpractical and *low-tech*) approaches such as specially-designed transparent plastic masks [13] or face painting (i.e., “adversarial computer vision” attack) [14]. However, these methods could be easily defeated as the advances in computer vision and face recognition are extremely fast, allowing correct identification through face recognition even when the subjects wear respiratory masks [15].

Another possible way is to develop, provide and use appropriate *high-tech tools* against the invasion of privacy by CCTV cameras. Examples of such tools include CCTV-aware route planning and navigation, and real-time early warning system when mobile and embedded devices that are video-input equipped (e.g., wearables, smartphones, drones) enter areas under the potential field of view of CCTV cameras. To this end, such tools require trustworthy object detection and counting, and accurate mapping and localization. In this context, computer vision is a proven method that excellently performs for object detection and counting [16], as well as for mapping and localization [17, 18]. However, in order to implement such CCTV-aware technology, various foundational blocks are currently missing. One such foundation block of utmost importance are object detectors for quick, accurate, and automated computer vision detection of CCTV cameras.

#### A. Extra motivation

Finally, in order to assess how serious is a privacy risk of a certain local/global CCTV installation is, certain modeling approaches require to identify and precisely count the CCTV cameras. Those models also require to know exactly where the cameras are located along with their other characteristics such as field of view, zoom levels, and other built-in features (e.g., face recognition, Infra-Red (IR), Pan-Tilt-Zoom (PTZ)). Unfortunately, most of the current data publicly available about CCTV cameras statistics and characteristics, both at global and local levels, can be considered *completely unreliable*. As follows, we provide several such examples that demonstrate the unsound methodologies and discrepancies in data. In one instance, the UK had until 2014 three different major estimations about the number of CCTV cameras – 1.8 mil. [19], 4.2 mil. [20], and 5.9 mil. [3]. To add insult to the injury, despite the rampant increase of CCTV and video surveillance globally, these numbers were not updated ever since, and are referenced in 2019–2020 as “current” by various reports and media outlets. In another instance, the estimates for global number of CCTV cameras vary between 25 mil. [21] and 770 mil. [4] – a whopping 25x discrepancy. In yet another instance, the UK finds that on average a person enters a CCTV camera view 300 times a day [21]. A similar study in the US puts that number at 50+ times a day, despite the more worrying fact that the average US respondent *assumed it was 4 cameras or less* [22] – at least a 10x lower presumed privacy risk and exposure than in reality. At the same time, a recent

journalist experiment in NYC (US) by Pasley [2] found he encountered CCTV cameras face-to-face at least 49 times, and that is *just counting a single trip to the workplace*. Finally, there are also discrepancies related to the number of cameras per 1000 persons [3, 19, 23]. A quick check reveals that such discrepancies may have several root-causes. In some cases, it is the use of unsound and low-tech methods, such as visually counting CCTV cameras on a *single main shopping street in London*, and then extrapolating (by some unvetted model) the numbers to the entire country [20]. In other cases, it is the heavy use of sales and marketing data [4], which by our experience very often is unrepresentative, highly approximated, and over-estimated. Even if we would assume the rightfulness of counting data provided by such unscientific methods, they cannot however provide the privacy-critical information about any camera, namely its location, characteristics (e.g., the field of view, zoom), and spatial coverage.

#### B. Contributions

In this paper, we try to close the existing fundamental research and technology gaps as well as to address the strong and imminent need for such tools. During the experiments on real-world data, our system achieved an accuracy of up to 98,7%, which is comparable to Google’s original automatic system for large-scale privacy protection of human faces and car license plates in Google Street View [24].

- We are the first to research, implement and evaluate Computer Vision (CV) models to detect *CCTV camera objects*<sup>1</sup> in images and video frames, with *particular focus on privacy and anonymity applications*.
- We are first to introduce and motivate a handful of *CCTV-aware applications and working prototypes* for both *mobile devices* and *privacy-first/safety-first routing* scenarios as relevant for modern digitized lifestyle.
- We release as *open data* the models and datasets necessary to validate our results and to further expand the datasets and the research field. To our knowledge, these are the first, the largest, and the best-performing datasets and models to be publicly released for solving the stated problems.
- The relevant artefacts (e.g., code, datasets, trained models, and documentation) will be available at: <https://github.com/Fuziih> and <https://etsin.fairdata.fi/dataset/d2d2d6e2-0b5c-46e0-8833-53d8a24838a0> (*urn:nbn:fi:att:258ce5ad-9501-46b9-a707-c1f59689ee10*).

#### C. Paper organization

The rest of this paper is organized as follows. We detail our methodology and describe our experimental setup in Section II. Then, in Section III we present our results and main findings. In Section IV we discuss the caveats, possible applications, and future work. In Section V we overview the related work. Finally, we conclude with Section VI.

<sup>1</sup>Our core aim at this stage is to be able to accurately detect *generally visible* CCTV cameras at a large-scale. Although our object detectors work well on certain edge-cases (Figures 4, 5), the camouflage attacks on object detectors (e.g., careful placement, decoration) is a separate emerging topic [25].

## II. METHODOLOGY AND EXPERIMENTAL SETUP

As with any Computer Vision (CV) object detector, we followed a two-phase approach. First, we trained multiple models for object detection using “training sets” (and additional “validation sets” for internal self-validation during model’s training). In order to train the CV object detectors, we split the phase into four parts – dataset gathering (Section II-A), image annotation (Section II-C), environment setup (Section II-E), and model training (Section II-F). Once the model training is completed, we evaluate each trained model against a “testing set”. Each dataset (see below, e.g., *Dataset0*, *DatasetAll*) had its own “testing set” which was withheld from the training and used only on finalized models as “in the wild” testing.

### A. Dataset gathering and definitions

When we started to gather the dataset, we made a practical decision that we want to be able to classify the cameras into at least two distinct sub-classes based on their shape – *directed cameras* and *round cameras*. Having this information allows us in the future work to model more accurately their field of view coverage in 3D, therefore allowing to decide whether a particular point in space (e.g., sidewalk, street, street corner) provides or not privacy to a person. However, it is important to note that, from the point of view of MS COCO annotations [26] and CV/ML training, we treat all the CCTV cameras as a single *camera* category, regardless of whether they are annotated as directed or round. This is in line with the MS COCO [26] approach, where for example, the *cars* category is represented as a single category regardless of the actual cars’ properties (e.g, shape, make, color).

*Directed cameras* include box- and bullet-shaped cameras (see Figure 15), and we assume such cameras record a limited field of view specifically in the direction they are pointed to. Some of them may be motorized (e.g., via Pan-Tilt-Zoom (PTZ) hardware and protocols) and therefore be able to have a mobile field of view (in theory up to 360°). However, it is challenging (if not impossible) to detect PTZ with computer vision on static (and low resolution) images. Therefore, to simplify a bit our experiments and future geo-mapping modeling, we assume that such cameras are static, cover the particular direction they are pointed to and have limited vertical and horizontal fields of view.

*Round cameras* include dome- and sphere-shaped cameras (see Figure 16), and we assume such cameras potentially record a 360° field of view. Even though some dome- and sphere-shaped cameras host inside a static and directed camera sensor, most of the times it is challenging to know that because of the reflective glass. Therefore, to simplify a bit our experiments and future geo-mapping modeling, we assume that such cameras record a 360° field of view.

To date, the collection, annotation, and quality-check of all the datasets presented in this paper took the equivalent of at least *five and a half person-months of effort*.

### B. Datasets overview

a) *Dataset0*.: Our first dataset, that we reference as *Dataset0*, was originally collected during January 2020 and February 2020 by contributor *Person0 HT* and later appended with more images from contributor *Person6 TL*. The images were collected from Flickr [27], 500px [28], Unsplash [29] and Google Maps Street View [30]. All the images in this dataset were annotated using Wada’s Labelme standalone annotation tool [31] by contributor *Person0 HT*. The *Dataset0* training set contained 3401 images with 3986 instances (2244 directed and 1742 round) and the validation set had 528 images with 617 instances (348 directed and 269 round) respectively. The *Dataset0* also featured a small testing set of 186 images with 231 instances (126 directed and 105 round) <sup>2</sup>.

For the *Dataset0* we trained the following models: Centermask2 [32] (backbone variants: VoVNet V2 Lite-39, 50 and 99), ATSS [33] (backbone variants: ResNet-50, ResNeXt-101), and TridentNet [34] (backbone variant: ResNet-101). Excellent performance of this early and original *Dataset0* could already be observed, as detailed in Appendix in Tables IX, X, XI.

After several rounds of peer-review rejections and comments, it became clear that the security and privacy community insists our *Dataset0*, is too small (hence not representative) despite its novelty and good performance. Therefore, we set ourselves on a quest to collect a dataset large enough that reaches, or even exceeds, the median size for a given object category as set by state-of-the-art computer vision works. MS COCO is a definitive state-of-the-art work which is a reference point for datasets related to object detection by computer vision. It contains 80 annotated object categories representing 860001 annotated object instances. In MS COCO, the median size of the training set per detected object category is 6097. Therefore, as detailed below we collected several more incremental datasets atop *Dataset0*.

b) *Dataset1*.: As our most immediate goal is to detect cameras from street-level imagery, our next effort to improve the dataset was to focus on dataset’s content to street-level imagery. Therefore, *Dataset1* only included the street view images from *Dataset0* with some new images from contributor *Person6 TL* that were captured during May 2020 from Google Street View [30]. All the new additions were also annotated using Wada’s Labelme standalone annotation tool [31] by contributor *Person0 HT*. The *Dataset1* training set contained 2457 images with 3101 instances (1554 directed and 1547 round) and the validation set had 270 images containing 354 instances (178 directed and 176 round). The testing set stayed the same as with *Dataset0*.

c) *Dataset2*.: The *Dataset2* was collected during late September 2020 using a crowd-sourcing effort by eight (8) contributors. For this, we used a custom developed annotation tool (see Section II-C). This dataset contains 4167 images with 5380 camera instances (3325 directed and 2055 round). The images were captured mostly from Google Street View [30],

<sup>2</sup>Later on, this testing set was however replaced with improved alternatives.

but Flickr [27] and Baidu Maps [35] were also used. This dataset was never used “*as is*” for model training and evaluation. However, all of the images captured in this dataset were used to create the training, validation and testing sets of our most complete dataset `DatasetAll` that we detail below.

*d) DatasetAll.*: Our latest and most complete dataset is `DatasetAll`. It was obtained by “merging” `Dataset0`, `Dataset1`, `Dataset2`, and applying de-duplication, cleanup and quality check after the merging process. It is important to note that due to the complex nature of the above process, the counts in `DatasetAll` are not just a plain sum-up of all the individual counts from `Dataset0`, `Dataset1`, `Dataset2`. After the “merging” process is completed, the `DatasetAll` training set contains 8387 images with 10419 camera instances (6137 directed and 4282 round), while its validation set has 533 images with 647 camera instances (379 directed and 268 round). We used `DatasetAll` to train our most recent models, namely “ResNeSt-200” and “DetectoRS: Cascade + ResNet-50”.

### C. Image annotation

Since we use supervised training at this stage, we have to label and annotate the images in our datasets.

*a) Dataset0, Dataset1.*: To annotate the images in these datasets, we used standalone deployed Wada’s Labelme tool [31]. Labelme is heavily inspired by the work by Russell et al. [36] who created LabelMe – web-based image annotation and labeling tool that operates in the browser but which requires the images to be uploaded and managed on own backend server, i.e., cannot annotate the images directly displayed in the browser while browsing third-party sites. Wada’s Labelme [31] allows annotation with polygon segments that can be used in object segmentation architectures such as Mask-RCNN [37] and CenterMask [32]. When using object segmentation, the outlines of the objects can be identified more precisely instead of a mere bounding box around the object of interest. Also, Wada’s Labelme outputs individual JSON files for each annotated image, and includes Python scripts to embed the data as a single annotation file in MS COCO format [31].

*b) Dataset2.*: Standalone tools such as Wada’s Labelme [31] come with high-overhead and high-maintenance costs, and are not the best suited for distributed crowd-sourcing efforts. To enable fast and easy crowd-source contribution, we have designed and developed from scratch a novel annotation tool implemented as an extremely flexible and COCO-compatible *browser-only extension*. Aiming at one-click solutions, it requires minimal setup and configuration effort, and is ready to use out of the box even by novice contributors. The browser extension is written in JavaScript and comes with a set of more than 10 distinctive features. To date, it took the equivalent of at least *five person-months of effort* to design, develop, test, and improve our browser-only annotation tool. As part of a separate publication, we describe the implementation details as well as its validation results, and we are releasing the tool under the open-source license.

*c) Post-annotation.*: Where needed and applicable, we annotated the final versions of our datasets (i.e., training, validation, testing) with polygon shapes, and converted those datasets to MS COCO-compatible format. We also saved the individual JSON annotation files for future reference. For example, they may be useful when annotation changes are needed, or when a different splitting of the dataset into training and validation subsets is required.

### D. Datasets details

TABLE I: Comparison: our datasets vs. MS COCO 2017.

Dataset Name	Total Categories	Total Instances	Median Instances per categ.	Increase (vs. Median MS COCO)
MS COCO (train)	80	860001	6097	1x
<code>DatasetAll</code> (train)	1	10419	<b>10419</b>	<b>1.70x</b>
<code>Dataset0</code> (train)	1	3986	3986	0.65x
MS COCO (val)	80	36781	265	1x
<code>DatasetAll</code> (val)	1	647	<b>647</b>	<b>2.44x</b>
<code>Dataset0</code> (val)	1	617	617	2.32x

TABLE II: High-level statistics for the datasets (training set).

	<code>Dataset0</code>	<code>Dataset1</code>	<code>Dataset2</code>	<code>DatasetAll</code>
Total counts				
Total collected images	3401	2457	4167	8387
Total annotated camera instances	3986	3101	5380	10419
Images grouped by source				
Google (Street View, Images Search)	1906	2457	3873	6598
Baidu street view	-	-	269	269
Flickr	935	-	25	960
500px	482	-	-	482
Unsplash	78	-	-	78
Instances grouped by sub-type				
Directed camera instances	2244	1554	3325	6137
Round camera instances	1742	1547	2055	4282
Instances grouped by pixel area				
Small ( $\leq 32 \times 32$ px)	685	762	1455	2331
Medium ( $32 \times 32 - 96 \times 96$ px)	2247	2147	3345	6397
Large ( $\geq 96 \times 96$ px)	1054	193	580	1691

### E. Environment setup

*1) Hardware.*: Object detector training requires a lot of system resources, especially with the larger backbones and with increasing dataset sizes. We trained our models on a supercomputer cluster that is part of a National Super Computing Grid. The supercomputer we used in our experiments employs 682 CPU nodes and its performance can theoretically peak at 1.8 petaflops. Each node has two 20 core Intel Xeon Cascade Lake processors running at 2.1 GHz. It also features an “AI partition” that includes 80 GPU nodes with four Nvidia Tesla V100 32GB GPGPUs each, totaling 320 GPGPUs. The total theoretical performance of the GPGPUs is 2.7 petaflops. The nodes carry 384 GB of main memory and 3.6 TB quick local storage. For our experiments, we used one node that employs four Nvidia Tesla V100 32GB GPGPUs. We also performed some intermediate tests on our group’s HPC GPU mini-cluster. It features two Intel Xeon E5-2640 v4 CPUs totaling 20 cores running at 2.40 GHz, and includes eight Nvidia Tesla P100



16 GB GPGPUs. For our experiments, we used four Nvidia Tesla P100 16GB GPGPUs.

2) *Software*: In Table III we present a detailed list of software used during our experiments. The majority of software in our experiments is based on (or is written in) Python, and the frameworks in our experiments were implemented in PyTorch. To work with HPC clusters, we also needed to set up a Python environment with several needed libraries and packages. In order to achieve the setup, a virtual environment is required. Therefore, we used Conda [38] which is an open-source virtual environment and package manager. Furthermore, Conda enabled us to install and use different matching versions of packages and libraries, and it also isolated them to the specific virtual environment, making the experimentation and failure less painful and more streamlined. In particular, we used Miniconda3 variant since we did not require the features of the bulkier Anaconda3 package.

TABLE III: Software and tools used to perform the experiments.

Software Name	Version	Purpose
Python	3.8.1	Python core
cuda toolkit	10.1.243	GPU programming
albumentations	0.4.3	Image augmentation library
numpy	1.18.1	Scientific computing package
OpenCV	4.2.0.32	Computer vision library
PyTorch	1.5.1	Machine learning framework
torchvision	0.6.1	Computer vision package
matplotlib	3.1.3	Graph visualizations
pycocotools	2.0	Tools for MS COCO
tqdm	4.42.1	Progress bar for terminal use
pillow	7.0.0	Imaging library (PIL fork)
cython	0.29.15	C-Extensions for Python
ninja	1.9.0	Small build system
pandas	1.0.1	Data analysis library
requests	2.23.0	HTTP library
scipy	1.4.1	Mathematics and science library
yacs	0.1.6	Configurations management system
Tensorboard	2.1.1	Training data capture
Detectron2	0.1.1	Object detection framework
mmcv-full	1.1.4	OpenMMLab Computer Vision framework
mmdet	2.2.0	MMDetection object detection toolbox
mmpycocotools	12.0.3	MMdet pycocotools fork
QCC	8.3.0	GNU Compiler Collection
CUDA	10.1.168	Nvidia CUDA
labelme	4.2.9	Annotation tool
ATSS		ATSS - detector
CenterMask2		CenterMask - detector (PyTorch)
TridentNet		TridentNet - detector
ResNeSt		ResNeSt - detector
DetectoRS		DetectoRS - detector
detectron2-pipeline		Modular image processing pipeline

## F. Model training

To date, it took the equivalent of at least *three person-months of effort* to perform all the model training experiments, including trials and failures as well as validation and testing of intermediate and final models. It also took the equivalent of at least *600 GPU-hours* of computing effort using the described hardware configurations.

1) *Initial models*: Our first efforts with `Dataset0` included three detectors with total of six varying models created. We trained CenterMask2 [32, 39] with VoVNet-V2 [40] as backbone using the *V-57-eSE*, *V-99-eSE*, *V-39-eSe* (*lightweight*) variants, ATSS [33], we used the ResNet-50 [41]

and ResNeXt-101 [42] backbones with multi-scale training and deformable convolutions and TridentNet [34] using the ResNet-101 [41] C4 backbone. As already mentioned, we achieved excellent results with our `Dataset0` where the highest precision was for validation set 95,6% and 91,1% for testing set respectively (see Section A). Though results were satisfactory, as our model use-cases began to realize and given the peer-reviews received, we decided to create a larger dataset with more variance in the images. As the field of object detection is evolving quickly, we also substituted our detectors for more promising ones. As our dataset has been overhauled including a whole new testing set and the metrics were modified to suit our needs also, the results are not entirely comparable. Therefore, we omit further comparison to the older models (`Dataset0`), and we focus entirely on our latest developments around `DatasetAll`.

2) *Latest models*: Therefore, for `DatasetAll` we used two state-of-the-art object detection frameworks to train our models with – FAIRs detectron2 [43] and MMDetection [44] by Multimedia Laboratory, CUHK. Our ResNeSt [45] model used detectron2 [46] and DetectoRS [47] model was trained on MMDet [44]. Both of the frameworks are equipped to handle our COCO-style dataset by default and feature dataset evaluators using the pycocotools library.

a) *ResNeSt*.: For ResNeSt [45], we chose a huge 200-layer deep backbone with the Cascade R-CNN [48] method. Most of the settings we left as standard at this point, therefore, the models feature FPN [49], SyncBN [50] and image scale variation that randomizes the short side of the input image between 640 and 800 pixels. We changed the class number to two and configured the training schedule in regards to our previous experiments in which we first set the maximum iterations to 45000 with (i.e., 0.5x of the “1x learning rate” schedule which translates to default 90000 iterations). However, we found that we get even better results at 20000–40000 iterations checkpoints. Therefore, our schedule was set to 36000 maximum iterations with lowering steps at 30000 and 34000 iterations. Our base learning rate was 0.02.

b) *DetectoRS*.: For DetectoRS [47], we chose the offered ResNet-50 based backbone. The images were input at 800 pixels short size and the learning rate was set at 0.01. The number of classes was set to two and the scheduler was left at 12 epochs. With our dataset and the setting at 2 samples per worker resulted in 4195 iterations per epoch totaling at 50340 iterations. The learning rate was stepped to one-tenth of the previous at the beginning of epoch nine and twelve.

## G. Various enhancements

1) *Image alterations*: We also propose and explore the effect of “image alteration” on the performance of our trained models [51]. As “image alterations” we applied auto-adjust to contrast, equalizer, exposure, and hue-saturation. Results improvement with “image alteration” vary across the models. DetectoRS did not show any signs of improvements on the false detections nor the confidence level increase. On the one hand, ResNeSt-model did turn a few False Negatives (FN) to

**TABLE IV:** Final configuration, iterations count, training and inference times, when training detectors on `DatasetAll`.

Detector	Best-result iterations (count [set])	Weights file size (MB)	Avg. train time / iter. (seconds [batch size])	Avg. inference time / 800px image (seconds)
ResNeSt	24999 [test] / 19999 [val]	1009	1.6 [batch 8]	0.171
DetectoRS	37750 (epoch 9) [test, val]	989	0.66 [batch 2]	0.13

True Positive (TP) and False Positives (FP) to True Negative (TN) when equalizer and exposure image alterations were applied. Still, plenty more tests need to be conducted in order to trust the altered images in the “production models” rather than the originals.

### III. ANALYSIS OF RESULTS

All the models were tested separately with both the validation dataset as well as with a separate testing dataset (see Section II-A). As mentioned earlier, the testing dataset mainly features images from street-level maps, since this corresponds to the intended use for the detector model. However, as shown in Section IV-A5 and Appendix A, our system performs well (94.6%) even with arbitrary images acquired by third-parties.

Tables IV and XI show the training iteration count for each model that provided the best performance for the whole training session. Additionally, these tables present the timings for training and inference under each detection model.

#### A. Metrics for evaluation

To evaluate our models, we used *pycocotools* and MS COCO evaluator built into the frameworks. For all the models trained, we used the same evaluator. The metrics we use and present are modified from the standard MS COCO’s [26] evaluation metrics to suit our goals. We present the modifications and the arguments for them. We also present a F1-score for our results, a metric derived from the average precision and recall. We measure our F1-score with 0.5 IoU and 100 detections per image thresholds. It gives equal emphasis on both types of false detections. We list the average precision per category (directed and round) as well. These metrics are not part of the standard COCO metrics suite. To evaluate the performance of a detector for the *detection performance*, MS COCO employs 12 characterizing metrics. *Average Precision (AP)* with MS COCO represents, in essence, a *mean Average Precision (mAP)* which takes the precision average across all the classes, all the while *localization accuracy* is built into the precision metrics. MS COCO’s standard measurement nowadays is largely represented by *Average Precision (AP)* and *Average Recall (AR)*, where the average is taken on 10 IoU thresholds from 0.5 to 0.95 with a 0.05 interval. AP across scales takes into account the area of pixels within the segmentation mask or the bounding box. In this context, based on the pixel size of the detected segmentation mask or the bounding box – “small objects” means areas up to  $32 \times 32$  pixels, “medium objects” fit areas between  $32 \times 32$  and  $96 \times 96$  pixels, and “large objects” are represented by areas beyond  $96 \times 96$  pixels.

We argue, that for our model use-cases (ie. detection from street view images), the “small objects” category is not representative or required. We argue that considering the varying quality of street view images, the resolution we want to run the images at and with computer collected images, objects under the  $32 \times 32$  pixel threshold are a subject for unnecessary false detections. Therefore, we omit the “small category” from our results and from further model uses, and we prefer to create a more intelligent image capturing algorithm to have good coverage over the captured streets. Our datasets still contain instances of the “small category” and the detection of them can be enabled or disabled at will. We also drift away from MS COCO with the average recall metrics. We argue that the number of detections past or below a certain reference point is not necessary as we only want the highest possible accuracy from our models. We set the maximum number of detections arbitrarily to 100 as it well past all our instances per image thresholds and should allow the models to perform.

With our main and immediate use-cases, the pixel-precise localization is not absolutely necessary, hence the precision with 0.5 IoU (i.e., AP@0.5 metric) is most relevant in our case. Therefore, we scale all of our results to the 0.5 IoU threshold.

#### B. Numerical results

In Table V we present the metrics (bounding box detection) for the “testing dataset” with 800-pixel short side images. The results are very good. The decision to cut the tiny samples from the detections is increasing our percentages greatly. Our F1 scores with both of our models are really high, which suggests the lack of false detections in the “larger detection categories”. Directed samples seem to be harder to detect in our “testing dataset”. We can also be happy about our localization accuracy as the tough 0.5:0.95 IoU category is in the 70-percentile range. Large samples are clearly no issue for our models and we can certainly suggest that our large sample size is adequate.

In Table VI we show the detection metrics (bounding box detection) for the “validation dataset”. The results are excellent. The scores are really high for all categories. Cross-referencing the “testing set” and “validation set” scores, we could argue a slight overfitting issue creeping in, especially with DetectoRS-model. In comparison, the directed subcategory also takes a hit in detection precision. Therefore, we will also argue, that our validation dataset needs yet another revision for improvement in detection generalization. As for now, we are extremely happy with all of the results including the tougher 0.5:0.95 IoU localization tests.

In Table VII we present the segmentation detection results for the ResNeSt-model. In comparison, we can see that the segmentation results are not far off from the bounding box results. In a few categories, the results are even slightly better. This suggests great localization precision and a great beginning for better identification for camera types as more accurate shapes can be detected as accurately than mere bounding boxes.

TABLE V: Results for bounding box detection with the DatasetAll testing set, 800px short side images, **bold**=best

Detector	AP@0.5	AP@0.5:0.95	APm	API	AR 100	ARm	ARI	F1	AP@0.5 (directed type)	AP@0.5 (round type)
ResNeSt	<b>92,0%</b>	<b>71,4%</b>	<b>91,5%</b>	<b>96,0%</b>	<b>94,5%</b>	<b>93,7%</b>	<b>100%</b>	<b>93,2%</b>	<b>89,2%</b>	<b>94,8%</b>
DetectoRS	91,5%	68,9%	91,1%	93,9%	93,1%	92,6%	95,5%	92,3%	89,1%	93,9%

TABLE VI: Results for bounding box detection with the DatasetAll validation set, 800px short side images, **bold**=best

Detector	AP@0.5	AP@0.5:0.95	APm	API	AR 100	ARm	ARI	F1	AP@0.5 (directed type)	AP@0.5 (round type)
ResNeSt	97,3%	80,1%	96,8%	98,7%	98,4%	98,0%	<b>99,6%</b>	97,8%	98,0%	96,5%
DetectoRS	<b>98,7%</b>	<b>83,4%</b>	<b>99,2%</b>	<b>98,8%</b>	<b>99,5%</b>	<b>99,7%</b>	99,1%	<b>98,5%</b>	<b>98,6%</b>	<b>98,7%</b>

TABLE VII: Results for ResNeSt segmentation detection with the DatasetAll testing and validation sets, 800px short side images

Set	AP@0.5	AP@0.5:0.95	APm	API	AR 100	ARm	ARI	F1	AP@0.5 (directed type)	AP@0.5 (round type)
Test	91,5%	70,2%	90,9%	96,2%	94,0%	93,2%	100%	92,7%	89,3%	93,8%
Val	97,0%	80,8%	96,5%	98,8%	98,1%	97,5%	99,6%	97,5%	97,3%	96,8%

Input image resolution is a debatable topic. Should we input images in their native resolution or at the training image size? The ideal case would obviously be if there was no discrepancy between the two. As our testing dataset contains slight higher resolution images than our testing set, we also tested the testing set with 1200 pixel short side input images. We present the results in Table VIII.

From the results, we can see that our DetectoRS-model clearly benefits from the increased input resolution achieving the highest scores with the “testing set“. However, our ResNeSt-model suffers from the increased input resolution and scores lower than with the smaller images. ResNeSt clearly benefits from images that are close to the training resolution. The results imply that testing the models with varying resolution is beneficial and keeping the resolution constant will yield the stable results we are after. As transfer-training these models is not that time-consuming, creating specialized models for each task (different image properties) is most likely beneficial.

### C. Visual result samples

To facilitate the understanding of successes, failures, and challenges faced by our detectors, we present in this section a selection of relevant samples along with some comments.

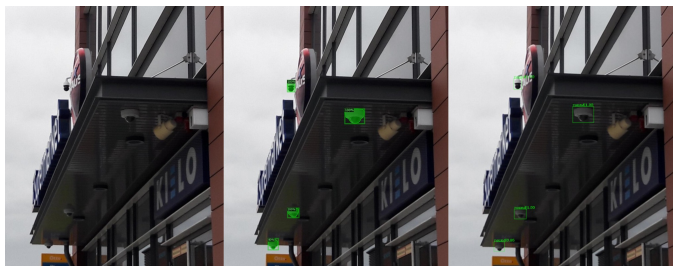


Fig. 1: Visual results (Ground Truth - 4 TP) (left to right): ResNeSt - 4 TP (3x100% and 80%); DetectoRS - 4 TP (3x100% and 95%)



Fig. 2: Visual results (Ground Truth - 4 TP) (left to right): ResNeSt - 4 TP (4x100%); DetectoRS - 4 TP (2x100%, 99% and 96%)

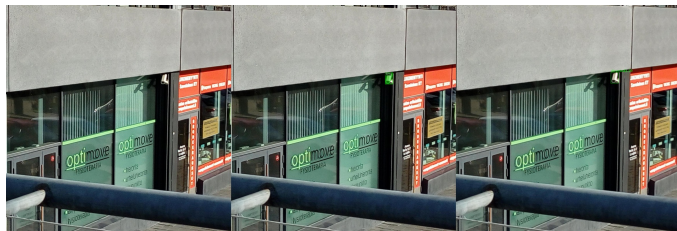


Fig. 3: Visual results (Ground Truth - 1 TP) (left to right): ResNeSt - 1 TP 99%; DetectoRS - 1 TP 100%

Figures 1, 2, 3 are perfect examples of our excellent results – all TP are found, and nothing else is detected. Also the confidence levels on these samples are really high (lowest is 80%).



Fig. 4: Visual results (Ground Truth - 1 TP) (left to right): ResNeSt - 1 FN; DetectoRS - 1 TP 95%

Figures 4 and 5 are examples on how DetectoRS edges out



TABLE VIII: Results for bounding box detection with the DatasetAll testing set, 1200px short side images, **bold**=best

Detector	AP@0.5	AP@0.5:0.95	APm	API	AR 100	ARm	ARI	F1	AP@0.5 (directed type)	AP@0.5 (round type)
ResNeSt	90,1%	71,9%	90,8%	87,0%	94,0%	93,7%	<b>95,5%</b>	92,0%	88,3%	92,0%
DetectoRS	<b>92,6%</b>	<b>72,8%</b>	<b>92,4%</b>	<b>93,3%</b>	<b>95,4%</b>	<b>95,3%</b>	<b>95,5%</b>	<b>94,0%</b>	<b>90,0%</b>	<b>95,2%</b>

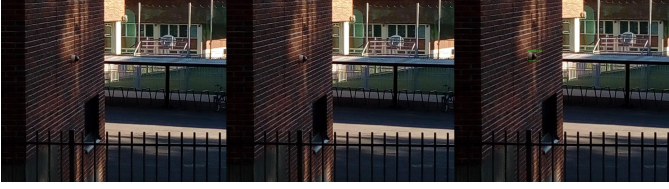


Fig. 5: Visual results (Ground Truth - 1 TP) (left to right): ResNeSt - 1 FN; DetectoRS - 1 TP 81%

on some of the samples. In Figure 4, the camera blends into the white wall in the sun and Figure 5 is quite dark. ResNeSt-model is unable to detect the cameras, but DetectoRS finds those and achieves good confidence in the TPs.



Fig. 6: Visual results (Ground Truth - 2 TP) (left to right): ResNeSt - 1 TP 99%, 1 FN; DetectoRS - 1 TP 99%, 1 FN

Figure 6 showcases a FN on both models. The directed camera in the upper corner of the image is undetected. However, the lower round-type camera is found in great confidence (99%).



Fig. 7: Visual results (Ground Truth - 2 TP) (left to right): ResNeSt - 2 TP (2x100%); DetectoRS - 2 TP (2x100%), 1 FN 74%



Fig. 8: Visual results (Ground Truth - 2 TP) (left to right): ResNeSt - 2 TP (2x100%), 1 FN 93%; DetectoRS - 2 TP (100% and 96%)

Figures 8 and 7 showcase on how the angle of the image can affect the results. Regardless of the angle, both models

find the TPs, but depending on the angle, both models find a single FP on opposite cases. Although, with ResNeSt, the confidence of the FP is quite high (93%) as in the DetectoRS case it is 74%, which could be rooted out with confidence limiting. Sensor fusion could also be used here for limiting the possibilities of FPs.



Fig. 9: Visual results (Ground Truth - 1 TP) (left to right): ResNeSt - 1 TP 88%, 2 FP (99% and 96%); DetectoRS - 1 FN, 1 FP 95%

Figure 9 is the worst sample on our “testing set“. ResNeSt finds two FPs on the two lamps present, but it also finds the camera. DetectoRS only finds a single FP. Confidence levels on the FPs are worryingly high.



Fig. 10: Visual results (Ground Truth - 2 TP) (left to right): ResNeSt - 2 TP (2x100%), 1 FP 78%; DetectoRS - 2 TP (100% and 99%), 1 FP 73%

In Figure 10, both models find the TPs easily with high confidence. However, both models also find a single FP with the lamp. The confidence of those FPs are still lower than usual (78% and 73%).

Next, we present some examples and results where we applied the “image alteration” techniques (Section II-G), thus seeking improvements in confidence levels and TP/TN/FP values that are as close as possible to the Ground Truth (GT).



Fig. 11: Visual results (Ground Truth - 1 TP) (left to right): Original - 1 FN; Contrast - 1 FN; Equalizer - 1 TP 73%; Exposure - 1 TP 79%; Saturation - 1 FN

Figures 11 and 12 showcase the result of “image alterations” on ResNeSt-model. In Figure 11, we find improvements as a FN is turned into a TP in exposure and equalizer



**Fig. 12:** Visual results (Ground Truth - 1 TP) (left to right): Original - 1 TP 88%, 2 FP (99% and 96%); Contrast - 1 TP 97%, 2 FP (99% and 96%); Equalizer - 1 TP 93%, 2 FP (99% and 80%); Exposure - 1 TP 65%, 1 FP 99%; Saturation - 1 TP 52%, 2 FP (96% and 92%)

tests. In Figure 12, the results are a mixed bag. On the exposure test, we remove a single FP, but the confidence level of the TP camera is hindered and still a single FP is present.

## IV. DISCUSSION

### A. Practical applications

1) *Fast and accurate CCTV camera annotations:* Crowd-sourcing is a proven and effective method for fast, accurate, and cost-effective for image labeling and annotation, and generic computer vision and machine learning tasks [52, 53, 54, 55, 56]. Google is using a similar approach integrated into its reCAPTCHA V2 [57, 58]. In Figure 19, we show our vision to extend the current reCAPTCHA V2 system. Our proposed improvement could ask the users of reCAPTCHA to “*Select all images with CCTV cameras*”, hence leveraging reCAPTCHA’s unified infrastructure and algorithms to better and faster help to annotate and validate the CCTV camera objects in Google Street View imagery as well as other image datasets. To our knowledge, at the time of this writing there is no such publicly available feature in Google’s reCAPTCHA.

2) *Global and instant mapping of CCTV locations and areas:* On the one hand, at present there are multiple projects and data-sources that provide the geo-location mapping of CCTV cameras. Some of these projects are open-source and crowd-sourced [59, 60], while some others are open-data resources provided by city administrations and country governments [61, 62, 63, 64]. However, all of these feature a set of major limitations, as follows. First, all these approaches cover a very limited geographical area (e.g., maximum a city). Second, the data-sources and projects are globally uncoordinated. Therefore the data formats along with the exposed characteristics of the respective maps and CCTV cameras vary dramatically across the board. Third, the crowd-sourced project relies heavily on human contributions of data, while governmental data-sources rely on human administration of data. Such an approach is highly unscalable for maintenance and development of the datasets, and exposes the data to human error and (un)intentional manipulations. Fourth, those datasets are rarely kept up-to-date and they inherently cannot reflect the instant changes in the addition, removal, reposition of CCTV cameras (e.g., due to infrastructure changes, construction).

On the other hand, our CCTV camera object detector can be applied to a global source of street-level imagery such as Google Street View, OpenStreetCam and, Mapillary. This allows fast mapping and localization of most street-level (and

even indoor<sup>3</sup>) CCTV cameras, therefore instantly creating and maintaining a global up-to-date (and historical [66]) map of CCTV cameras. At the same time, our CCTV camera object detector can be used to validate the accuracy and truthfulness of the crowd-sourced and open-data datasets. To achieve this, an automated process picks each CCTV camera entry from a dataset, retrieves the relevant and closest street-level and geo-tagged imagery, applies our CCTV camera object detector, and finally validates if the dataset is correct and contains up-to-date information.

3) *CCTV-aware route planning and navigation:* Once the CCTV cameras can be accurately detected, and instantly located and mapped based on street-level imagery<sup>4</sup> (see Section IV-A2), the system is ready for one of the most important and relevant application – *CCTV-aware route planning and navigation*.

At present, there is a myriad of route planning algorithms, software, and services<sup>5</sup> [67, 68, 69, 70, 71, 72]. However, to the best of our knowledge, none of the currently available algorithms, software, and services provide *CCTV-aware* route planning and navigation. To the best of our knowledge, we are the first to propose and work on such features at present and we are unaware of any project or service developing or offering such route planning options.

In Figures 13, 14, 21, 20 we demonstrate some real-world use-cases of such a CCTV-aware route planner. The samples contain the mapping and labeling of location, type (e.g., *round camera*, *directed camera*), and field of view. This mapping and labeling is achieved using the previously detailed CCTV camera object detectors (Sections II, III). The user first have the option to select the type of *CCTV-aware routing*, as presented for example in Figure 18.

If the user selects the “*Follow CCTV Cameras (safety-first)*” option, the system would provide a route as in Figures 13, 21. As already mentioned, current route planning solutions provide *CCTV-unaware* algorithms, therefore the systems we tested such as Google Maps, OpenStreetMap (OSM), by default provided almost always non-privacy-preserving routes (e.g., Figures 13, 21).

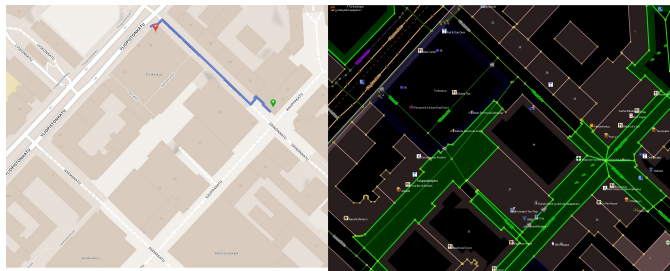


**Fig. 13:** Excerpt from our **working prototype**: default route is shown as obtained with OSRM as a core routing engine – CCTV-aware customization and cameras locations disabled.

<sup>3</sup>Our approach can also detect and map indoor CCTV cameras thanks to panoramas in Google Street View supplied by Google and its users [65].

<sup>4</sup>Also can be applied to geotagged photos and videos.

<sup>5</sup>A wide variety of open-/closed-source, online/offline, free/paid solutions.



At the same time, with our *CCTV-aware* route planning proposal, the user may alternatively select “*Avoid CCTV Cameras (privacy-first)*”. Therefore, our system would provide a better route for that scenario, as shown in Figures 14, 20.

Below we shortly explain the main excerpts taken from working prototypes. In Figure 14 (right), we enabled the CCTV-aware customizations and placed some “round cameras” on the map representing some real-life cameras and their actual positions as collected and mapped in a city that is covered by our system. Compared to Figure 13 (right), there are now at least four “round cameras” between starting and ending route points (highlighted within the red area) as shown in Figure 14 (right). Given this configuration, we enabled the CCTV-aware customizations in our prototype Open Source Routing Machine (OSRM) backend [73]. As expected, in Figure 14 (left) it produced an acceptable *privacy-first* routing that is different from the default OSM/OSRM routing in Figure 13 (left). Also as expected, the *privacy-first* routes may not necessarily be optimal in terms of travel distance or time. Indeed, increased travel time and distance is one of the trade-offs a person may need to accept in order to benefit from *privacy-first* routing.



**Fig. 14:** Excerpt from our **working prototype**: CCTV-aware routing system providing route for “*Avoid CCTV Cameras (privacy-first)*” user option – CCTV-aware customization and cameras locations enabled.

At a very high-level, our **working prototype** of CCTV-aware map routing and navigation uses the following components:

- **OSM:** access to global mapping and street data, and programmatic APIs to access and manipulate its data
- **OSRM backend:** efficient route calculations based on various constraints – we model CCTV cameras’ areas of coverage as certain type of constraints in OSRM
- **OSRM frontend:** UI/UX and testing/validation of routing and navigation correctness
- **JOSM editor:** visualization, editing, and debugging of routing and CCTV data
- **Street widths data:** location-specific data – this may affect CCTV coverage over a particular route

Due to space constraints and the depth of the topic, we leave the detailed presentation and evaluation of our *CCTV-aware privacy-/safety-first route planning and navigation* for one of the upcoming publications.

4) *Real-time CCTV detection on mobile/IoT devices:* Finally, one more application of the presented object detector is its use for real-time CCTV camera detection on smartphones,

mobile equipment (e.g., robots, drones), and other IoT/edge devices (e.g., RaspberryPi, ESP32-cam, Nvidia Jetson). For this purpose, our object detectors are configured and trained for low-power devices using, for example, TinyML hardware with TensorFlow Lite [74, 75], or variants of the state-of-the-art MobileNet [76, 77, 78], and GhostNet [79, 80].

One use-case could be drones or mobile robots equipped with tiny/lite versions of our detection models could move around the corner or down the street to first detect and map the CCTV areas (i.e., data collectors). The device would then alert the user when it detects in real-time a CCTV camera in its field of view, therefore providing the user a chance to change course and make a more informed decision.

At present, we are experimenting with several variants of *CCTV-aware mobile devices*, such as the ones based on RaspberryPi4 (RPi4) and Nvidia Jetson Nano. Figure 22 presents one of our RPi4 prototypes that we built for our complete CCTV-aware experimental set. Our RPi4 prototype is equipped as follows. One PiCamera (mounted on the Pan-Tilt HAT) provides both image/video acquisition (e.g., up to real-time 24-30 FPS if needed). One Coral USB provides AI/ML acceleration to enable real-time object detector loaded and running as lightweight model within Google’s Coral chipset. One GPS-dongle is for accurate localization of the device (e.g., 5–10 meters with GPS II chipsets). One programmable UART/TTL laser-based range finder (mounted on the Pan-Tilt HAT) enables very accurate ( $\pm 2\text{mm}$  error at 60m range) distance measurement to the detected CCTV cameras. One Pan-Tilt HAT enables PiCamera movement for centering and focusing the PiCamera street imagery or on detected CCTV cameras, as well as the movement of the UART/TTL laser-based range finder. At a very high level, the principle of operation of one such device mounted on backpack, helmet, bicycle, car rooftop/windshield, is presented in Listing 1. In our experiments, the maximum drawn power consumption for the entire prototype was 7W, i.e., 1.4A at 5V RPi4 supply. For example, using a standard yet high-performance powerbank of 30000mAh, it could operate around 20–24 hours.

Due to space constraints and the depth of the topic, we leave the detailed presentation and evaluation of our *mobile device CCTV-aware camera detectors and data collectors* for one of the upcoming publications.

5) *Validation on third-party data in real-life:* In this context, we also tested our system (namely the ATSS X-101 and Trident R-101 models) against the real-world journalist experiment by Pasley [2], where the “ground truth” consists of 39 TPs (i.e., CCTV cameras). Running ATSS X-101 detector resulted in 33 TPs + 0 FPs + 6 FNs. Applying Trident R-101 model produced 33 TPs + 1 FPs + 6 FNs. Both models presented an F1-score of 91.7%, and while their TPs and FNs counts are the same, the actual distribution of TPs and FNs across the input images slightly differ. Therefore, we also evaluated our system using a “sensor fusion” approach [81], where the best results from both the detectors (i.e., “sensors”) are combined (i.e., “fused”) together for an enhanced final result. In this case, our system achieves 35 TPs + 0 FPs + 4

FNs with an F1-score of 94.6%. A visual results subset from our experiment can be seen in Appendix A. This, therefore, underpins once again that our technology could be useful as *privacy-first* early warning system against CCTV cameras for real-life use by third parties and users.

### B. Technical challenges

Based on our real-world and street imagery observations, light equipment (e.g., light poles, light fixtures) many time look very similar to CCTV cameras. This makes it challenging to certainly distinguish between CCTV cameras and light equipment even to an experienced human observer. The worst-performing sample in our “testing set” is Figure 9 where the FPs are in fact round lamps or light fixtures. It is a perfect example that such a scenario poses certain challenges. Most of the FPs resulted where “small” size TPs were present. However, FPs resulted also for a small number of TPs of “medium” and “large” sizes, for example shapes on walls where the light hits the wall just at specific angle. These types of FPs will happen, and the way to root them out is possibly to use more intelligent image capturing and some sensor fusion techniques. At the same time, there is a growing trend to have streetlights with embedded CCTV cameras [82]. We suspect this may pose additional challenges (not insurmountable though) for the most accurate detection of CCTV cameras in real-life scenarios.

### C. Ethical aspects and potential abuse

On the one hand, there are less technological domains where a system inspired by our work could be applied. For example, the case of Novichok (A-234) poisoning in Salisbury (UK) of the former Russian military intelligence officer Sergei Skripal, and his daughter Yulia Skripal, by what is believed to be two officers of Russian GRU [83, 84], is surreal and beyond infamous [85]. Following the attack and the international diplomatic fallout featuring sanctions and diplomatic expulsions, the Law Enforcement agencies and investigative think-tank organizations (e.g., Bellingcat) reconstructed the complete routes with exact geo-positions, timestamps, and visual proof of main suspects *with the heavy use of state- and privately-owned CCTV cameras* [86]. In this context, some readers may object that future potential delinquents could use a system similar to ours in order to map the CCTV cameras within a planned operation area (if not already available), and then use it to carefully generate a specific route that provides close to 100% anonymity. We argue our point of view on this at the end of this section.

On the other hand, there are offensive cybersecurity scenarios (possible but unlikely in the immediate future), where our technology could be potentially used.

**Attack description:** The scenario works under the following attack assumptions:

- it is completely autonomous (i.e., *no human operators*)
- it involves offensive drones equipped with CCTV camera object detector (*attackers*) (see Section IV-A4)
- it targets highly-valuable air-gapped network(s) to exfiltrate data from (*victims*)

The drones use the object detector to identify CCTV cameras and approach them. Once approached, the drones would send a “backdoor knock” signal (e.g., visual, sound, infra-red) to the camera [6, 87]. If a particular CCTV camera was internally compromised and connected to an isolated network segment that contains a latent malware implant (e.g., APT), the malware activates when the camera receives the “backdoor knock” signal. The malware could also be implanted in the CCTV camera itself via IoT malware and firmware modifications [7, 88, 89]. To complete the attack, the drones with such CCTV camera object detection and data-exfiltration capabilities follow the *air-jumper* attack described by Guri and Bykhovsky [87].

All in all, we argue that while our CCTV camera object detector is designed to be used for *positive impact*, the potential of our proposed system being misused is similar and comparable to any other system (e.g., Kali Linux, Metasploit), method (e.g., penetration testing, reverse engineering), or device (e.g., kitchen knives in supermarkets). Additionally, we argue that the benefits of our system for the majority of *positive impact* applications outweigh the risks of misuse for a fraction of *negative impact* applications (where we believe the perpetrators to be able to find other ingenious ways for illegal or unethical activity, should a system like ours not exist).

## V. RELATED WORK AND STATE OF THE ART

### A. Object detection systems

1) *Detectron2*: Detectron2 [43] is “*Facebook AI Research (FAIR)’s next generation software system that implements state-of-the-art object detection algorithms*”. It is a complete rewrite of the open source object detection platform Detectron [90], and originated from FAIR’s successful maskrcnn-benchmark project [91]. FAIR suggests that the modularity of the framework grants the users flexibility and extensibility to train and use state-of-the-art object detection algorithms with various system configurations ranging from single GPU PCs to multi-GPU clusters [43].

2) *ResNeSt*: ResNeSt - Split-Attention Networks was introduced in April 2019 by H. Zhang et al. [45]. It features a novel building block to improve the standard ResNet backbone structure, which was originally developed for image classification rather than object detection. The authors introduce their modular Split-Attention block to enhance the performance of the ResNet architecture and gear it towards more downstream object detection and segmentation tasks. Their ResNeSt network consists of multiple Split-Attention blocks stacked to the ResNet structure. In general, each Split-Attention block divides the feature maps into subgroups. The feature representation of the group is derived from a weighted combination of even smaller feature divides called splits. [45]. Zhang et al. [45] showcase their state-of-the-art results using the ResNeSt backbone on Cascade RCNN [48] -model.

3) *MMDetection*: MMDetection is a rich object detection toolbox created by K. Chen et al. [44]. It is a highly efficient and modular state-of-the-art toolset featuring lots of frameworks and it is running on the back of PyTorch. It features object detection and instance segmentation tools and authors

claim state-of-the-art training speeds. It also won the 2018 COCO Challenge object detection section. [44]. Their paper submission for the public was in June 2019 and currently MMDetection is in version 2.

4) *DetectoRS*: DetectoRS paper was released in June 2020 by S. Qiao et al. [47]. It features two distinct mechanisms to improve on object detection tasks. They propose Recursive Feature Pyramid (RFP) on top of regular FPN [49] structure. RFP features increased feedback connections from the FPN [49] to the bottom-up backbone layers in turn adopting “looking and thinking twice” design. The authors explain that this creates more powerful feature representations [47]. Another distinct feature of the DetectoRS is the Switchable Atrous Convolution (SAC). It enables the backbone to conditionally adapt to different scales of objects. The gist of SAC is that it doesn’t require retraining of previous weights as it can adapt the standard convolutions to conditional convolutions effectively [47]. To date, DetectoRS using the ResNet-50 and ResNeXt-101-32x4d backbones achieves state-of-the-art results in COCO test-dev tasks [47].

### B. Object detection datasets

Lin et al. [26] proposed a novel dataset for general object detection called Microsoft’s Common Objects in COntext (COCO, or MS COCO). The most recent (2017) update of MS COCO has a fully annotated training dataset containing 118000 images and a 5000 image validation dataset. In addition, a 41000 image testing dataset is also available. There are more than 80 different classes for state-of-the-art object detector testing with the MS COCO [92], including pedestrians, traffic lights, cars, and even teddy-bears. However, it does not contain object detection models for CCTV cameras, though they are currently an indispensable part of any street and city infrastructure such as traffic lights and road signs.

PASCAL Visual Object Classes (VOC) [93] project ran object detection challenges between 2005–2012 [94]. For the 2012 challenge, PASCAL VOC dataset labeled 20 classes with both training and validation sets, and provided more than 11000 images totaling over 27000 instances [95]. The dataset contained several similar classes to increase difficulty [96].

ImageNet Large Scale Visual Recognition Challenge (ILSVRC) [97] is an ongoing annual object category classification and detection challenge that has been run since 2010. Russakovsky et al. [97] envisioned ILSVRC to follow PASCAL VOC [93] footsteps in providing a challenging dataset and hosting competitions. ImageNet provides about 1.2 million images for training and around 150000 images for validation and testing. ImageNet has 1000 classification labels, 200 being originally chosen for object detection challenges [97].

Open Images Dataset V6 contains over 9 million annotated images for a total of more than 15 million bounding boxes covering about 600 object classes [98]. The project holds the annual Robust Vision Challenges, and its goal is to further improve the development of computer vision systems [99].

In this context, our work is novel and perfectly extends the state of the art by contributing both the methods (e.g.,

code, scripts), as well as annotated data and trained models necessary for object detection of two classes of CCTV cameras (directed and round – see Section II-A).

### C. Computer vision / object detection on street-level imagery

There are numerous companies and projects capturing and serving street-level imagery such as Google Street View, EveryScape, Mapjack, Microsoft StreetSide, Yandex Street Panoramas, OpenStreetCam, Mappillary. Such imagery allows much richer online and offline experiences boosted by technological advances in Computer Vision (CV), Machine Learning (ML), Natural Language Processing (NLP) with text mining, Virtual/Augmented/eXtended Reality (VR, AR, XR). Overall, capturing street-level imagery presents both tremendous challenges and opportunities [100].

Paiva [101] used “*computer vision to infer urban indicators on google street view*”. Wojna et al.[102] presented a method for “*extraction of structured information from street view imagery*”. Hara et al. [103, 104, 105, 106] used “*google street view using crowdsourcing, computer vision, and machine learning*” for an extensive set of detections and challenges related to street-level accessibility for persons with special needs. Frome et al. [24] presented methods for large-scale privacy protection in Google Street View imagery. Using their fully automatic system the authors were “*able to sufficiently blur more than 89% of faces and 94–96% of license plates in evaluation sets sampled from Google Street View imagery*”. Related to the accurate mapping of an image based on street-level imagery, Zamir and Shah [107] introduced methods for image localization using Google Street View with an accuracy comparable to GPS-based technology.

However, none of the existing works attempted to perform detection and accurate location mapping of CCTV camera objects from street-level imagery. In this context, our work is the first to achieve this and perfectly extends the state of the art by accurately detecting CCTV cameras on both street-level and other imagery (both geotagged and not).

### D. Face recognition, privacy and CCTV

Face recognition is a very hot topic, has been a prolific area of research, and there is an immense body of works [108, 109, 110, 111, 112, 113, 114]. At the same time, (near) real-time face detection, tracking, and recognition is one of the core applications of CCTV cameras which is increasingly gaining traction. Several papers have been released on the subject of facial detection and recognition in real-time recordings such as the ones in CCTV setups. Halawa et al. [115] recently showed how the *Faster R-CNN* [116] algorithm is used with face detection in CCTV systems. Bah and Ming [117] presented their facial recognition algorithm. Their method includes pre-processing the images to better capture facial features and then implementing their own Local Binary Pattern (LBP) algorithm [111]. Mileva and Burton [118] demonstrated the use of facial recognition in a noisy real-life environment such as in CCTV camera footage. The authors conclude that facial recognition from CCTV footage is certainly an arduous task



and prone to errors [118]. Worse, erroneous face recognition results may lead to arrests of innocent persons, multiple times the arrests were found to be wrong [119].

However, large CCTV networks may provide unaccountable access to their video streams, turning them into tools of *illegal mass surveillance* [120]. Additionally, the researchers were able for a fee to get access to the “*face search*” feature, where the requestor provides a photo containing a “reference face”. Then, the facial recognition sub-system of the CCTV network provides back an extensive list of exact geo-locations (and other meta information) where similarly matching faces were previously seen within the CCTV network. The access to video feeds and to the “*face search*” feature is allegedly sold for a very low fee on underground and specialized forums by unscrupulous law enforcement officers (i.e., a particular instance of the *insider threat* [121, 122]).

In this context, our research, through the automated CCTV camera detection (having as immediate goal accurate mapping of camera geo-locations and characteristics) aims to provide users with tools for a more democratic use of technology where privacy controls are on the users’ side. For example, such tools may help the users to make an informed and real-time decision whether they want to be (or not!) in an area within the field of view of CCTV cameras.

#### E. Cybersecurity and CCTV/IP cameras

Recent research demonstrated that the state of cybersecurity for IoT devices (including DVRs and CCTV/IP cameras) and their firmware is very bad [123, 124, 125]. Back in 2013, independently and almost simultaneously Heffner [126], Costin [127], Shekyan and Harutyunyan [128] researched and presented about vulnerabilities, exploits and cybersecurity dangers related to vulnerable and exposed CCTV/IP/surveillance cameras. In particular, [127] proposed several hypotheses related to (in)security of CCTV/IP cameras, which were later extended and systematized in [6]. Unsurprisingly, in 2013–2014 reports started to surface about the infamous (and supposedly Russian-operated) Insecam project [129, 130], which at its peak featured between 100-200k video feeds from vulnerable/insecure CCTV/IP cameras connected to the internet. Moreover, in late 2016 news broke about the infamous and devastating Mirai IoT botnet [7, 131]. It featured the largest known DDoS attacks to date of over 1 TB/s, employed at peak about 600k devices, took down major parts of the internet, and mostly consisted of hacked CCTV/IP cameras and CCTV/DVR surveillance systems.

While this work does not explicitly address the cybersecurity of CCTV cameras, a possible offensive scenario is presented in Section IV-C.

## VI. CONCLUSION

In this paper, we presented the first computer vision object detectors aiming to accurately identify CCTV cameras in images and video frames. To build our system, we used and evaluated in parallel several state-of-the-art computer vision frameworks and backbones. To this end, our best detectors

were built using 8387 images that were manually reviewed and annotated to contain 10419 CCTV camera instances, and achieve an accuracy of up to 98,7%.

Furthermore, we develop and introduce by the way of preview and main excerpts, the first known and working prototypes of: a) *CCTV-aware route planning and navigation*; b) *CCTV-aware mobile devices* (data collection and real-time mapping); c) *Browser-only image annotation toolset*. These prototypes are motivated and powered by the core object detectors effort presented above. We presented excerpts and proofs of working prototypes, however we leave their detailed presentation as separate publications.

Finally, with this work, we hope to motivate in several ways the communities of researchers, practitioners, policy-makers, and end-users. First and more general is to focus the debates and policy-making related to privacy and safety of CCTV cameras towards a more science-, technology- and research-driven ground. Second is to encourage the improvement of our object detectors and techniques presented, so that they can be immediately incorporated at a larger scale, both in cloud and edge applications, and for the greater privacy benefit. With these in mind, we release the relevant artefacts (e.g., code, datasets, trained models, and documentation) at: <https://github.com/Fuziih> and <https://etsin.fairdata.fi/dataset/d2d2d6e2-0b5c-46e0-8833-53d8a24838a0> (*urn:nbn:fi:att:258ce5ad-9501-46b9-a707-c1f59689ee10*).

#### ACKNOWLEDGMENTS

We acknowledge grants of computer capacity from the Finnish Grid and Cloud Infrastructure (FGCI) (persistent identifier *urn:nbn:fi:research-infras-2016072533*). Part of this research was kindly supported by the “17.06.2020 *Decision of the Research Dean on research funding within the faculty*” grant from the Faculty of Information Technology of the University of Jyväskylä, and the grant was facilitated and managed by Dr. Andrei Costin. Authors would also like to thank the following persons for their dedicated efforts during the crowdsource data collection phase: Pyry Kotilainen, Janne Uusitupa, Arttu Takala, Syed Khandker, Anna Arikainen.

## REFERENCES

- [1] H. Turtiainen, "State-of-the-art object detection model for detecting CCTV and video surveillance cameras from images and videos," Master's thesis, University of Jyväskylä, Jyväskylä, Finland, 2020. [Online]. Available: <http://urn.fi/URN:NBN:fi:jyu-202005253430>
- [2] J. Pasley, "I documented every surveillance camera on my way to work in New York City, and it revealed a dystopian reality," <https://www.businessinsider.com/how-many-security-cameras-in-new-york-city-2019-12>, Dec 2019.
- [3] D. Barrett, "One surveillance camera for every 11 people in Britain, says CCTV survey," 2013.
- [4] E. Cosgrove, "One billion surveillance cameras will be watching around the world in 2021," <https://cnbc.com/2019/12/06/one-billion-surveillance-cameras-will-be-watching-globally-in-2021>.html.
- [5] A. Glinsky, *Theremin: ether music and espionage*. University of Illinois Press, 2000.
- [6] A. Costin, "Security of CCTV and video surveillance systems: Threats, vulnerabilities, attacks, and mitigations," in *6th International Workshop on Trustworthy Embedded Devices (TrustED)*, 2016.
- [7] M. Antonakakis et al., "Understanding the mirai botnet," in *26th USENIX Security Symposium (USENIX Security 17)*. USENIX Association, 2017.
- [8] Electronic Frontier Foundation, "Street-Level Surveillance – Surveillance Cameras," <https://www.eff.org/pages/surveillance-cameras>.
- [9] C. Slobogin, "Public privacy: camera surveillance of public places and the right to anonymity," *Miss. LJ*, vol. 72, p. 213, 2002.
- [10] B. v. S.-T. Larsen, *Setting the watch: privacy and the ethics of CCTV surveillance*. Bloomsbury Publishing, 2011.
- [11] J. Ryberg, "Privacy rights, crime prevention, cctv, and the life of mrs aremac," *Res Publica*, vol. 13, no. 2, pp. 127–143, 2007.
- [12] B. J. Goold, "Privacy rights and public spaces: Cctv and the problem of the "unobservable observer"," *Criminal Justice Ethics*, vol. 21, no. 1, pp. 21–27, 2002.
- [13] E. Heathcote, "Artists and activists offer privacy hope as facial recognition spreads," <https://www.ft.com/content/15fb3c5a-2178-11ea-b8a1-584213ee7b2b>, 2020.
- [14] M. Lothian-McLean, "These activists use makeup to defy mass surveillance," [https://i-d.vice.com/en\\_uk/article/jge5jg/dazzle-club-surveillance-activists-makeup-marches-london-interv](https://i-d.vice.com/en_uk/article/jge5jg/dazzle-club-surveillance-activists-makeup-marches-london-interv)
- [15] M. Pollard, "Even mask-wearers can be ID'd, China facial recognition firm says," <https://reuters.com/article/us-health-coronavirus-facial-recognition/even-mask-wearers-can-be-idd-china-facial-recognition-firm-says>
- [16] D. Onoro-Rubio and R. J. López-Sastre, "Towards perspective-free object counting with deep learning," in *European Conference on Computer Vision*. Springer, 2016.
- [17] J. Fuentes-Pacheco, J. Ruiz-Ascencio, and J. M. Rendón-Mancha, "Visual simultaneous localization and mapping: a survey," *Artificial intelligence review*, vol. 43, no. 1, pp. 55–81, 2015.
- [18] G. Verhoeven, M. Doneus, C. Briese, and F. Vermeulen, "Mapping by matching: a computer vision-based approach to fast and accurate georeferencing of archaeological aerial photographs," *Journal of Archaeological Science*, vol. 39, no. 7, pp. 2060–2070, 2012.
- [19] G. Gerrard and R. Thompson, "Two million cameras in the uk," *CCTV image*, vol. 42, no. 10, p. e2, 2011.
- [20] M. McCahill and C. Norris, "CCTV in London," *Report deliverable of UrbanEye project*, 2002.
- [21] "How Many CCTV Cameras in London?" <https://www.caughtoncamera.net/news/2021-many-cctv-cameras-in-london/>.
- [22] B. Karas, "Americans Vastly Underestimate Being Recorded on CCTV," <https://ipvm.com/reports/america-cctv-recording>.
- [23] P. Bischoff, "Surveillance camera statistics: which cities have the most CCTV cameras?" <https://www.comparitech.com/vpn-privacy/the-worlds-most-surveilled-cities/>.
- [24] A. Frome, G. Cheung, A. Abdulkader, M. Zennaro, B. Wu, A. Bissacco, H. Adam, H. Neven, and L. Vincent, "Large-scale privacy protection in Google Street View," in *12th international conference on computer vision*. IEEE, 2009.
- [25] L. Huang, C. Gao, Y. Zhou, C. Xie, A. L. Yuille, C. Zou, and N. Liu, "Universal Physical Camouflage Attacks on Object Detectors," in *Proceedings of the IEEE/CVF Conference on Computer Vision and Pattern Recognition*, 2020, pp. 720–729.
- [26] T.-Y. Lin, M. Maire, S. Belongie, J. Hays, P. Perona, D. Ramanan, P. Dollár, and C. L. Zitnick, "Microsoft COCO: Common objects in context," in *European Conference on Computer Vision*. Springer, 2014.
- [27] "Flickr," <https://www.flickr.com/>.
- [28] "500px.com," <https://500px.com/>.
- [29] "Unsplash.com," <https://unsplash.com/>.
- [30] "Google Street View," <https://www.google.com/streetview/explore/>.
- [31] K. Wada, "labelme: Image Polygonal Annotation with Python," <https://github.com/wkentaro/labelme>, 2016.
- [32] Y. Lee and J. Park, "Centermask: Real-time anchor-free instance segmentation," 2019.
- [33] S. Zhang, C. Chi, Y. Yao, Z. Lei, and S. Z. Li, "Bridging the gap between anchor-based and anchor-free detection via adaptive training sample selection," 2019.
- [34] Y. Li, Y. Chen, N. Wang, and Z. Zhang, "Scale-aware trident networks for object detection," 2019.
- [35] "Baidu Maps," <https://map.baidu.com/>.
- [36] B. Russell, A. Torralba, K. Murphy, and W. Freeman, "Labelme: A database and web-based tool for image

- annotation,” *International Journal of Computer Vision*, vol. 77, no. 1-3, pp. 157–173, 2008. [Online]. Available: <http://dx.doi.org/10.1007/s11263-007-0090-8>
- [37] K. He, G. Gkioxari, P. Dollár, and R. Girshick, “Mask R-CNN,” 2017.
- [38] “Conda — conda 4.8.3 documentation,” <https://docs.conda.io/projects/conda/en/latest/>.
- [39] Y. Lee and J. Park, “CenterMask2: Real-Time Anchor-Free Instance Segmentation,” Apr. 2020.
- [40] Y. Lee, J. won Hwang, S. Lee, Y. Bae, and J. Park, “An Energy and GPU-Computation Efficient Backbone Network for Real-Time Object Detection,” 2019.
- [41] K. He, X. Zhang, S. Ren, and J. Sun, “Deep Residual Learning for Image Recognition,” 2015.
- [42] S. Xie, R. Girshick, P. Dollár, Z. Tu, and K. He, “Aggregated Residual Transformations for Deep Neural Networks,” in *Conference on Computer Vision and Pattern Recognition*. Honolulu, HI: IEEE, 2017.
- [43] Y. Wu, A. Kirillov, F. Massa, W.-Y. Lo, and R. Girshick, “Detectron2: A PyTorch-based modular object detection library,” <https://ai.facebook.com/blog/detectron2-a-pytorch-based-modular-object-detection-library/>.
- [44] K. Chen, J. Wang, J. Pang, Y. Cao, Y. Xiong, X. Li, S. Sun, W. Feng, Z. Liu, J. Xu, Z. Zhang, D. Cheng, C. Zhu, T. Cheng, Q. Zhao, B. Li, X. Lu, R. Zhu, Y. Wu, J. Dai, J. Wang, J. Shi, W. Ouyang, C. C. Loy, and D. Lin, “Mmdetection: Open mmlab detection toolbox and benchmark,” 2019.
- [45] H. Zhang, C. Wu, Z. Zhang, Y. Zhu, Z. Zhang, H. Lin, Y. Sun, T. He, J. Mueller, R. Manmatha, M. Li, and A. Smola, “Resnest: Split-attention networks,” 2020.
- [46] Y. Wu, A. Kirillov, F. Massa, W.-Y. Lo, and R. Girshick, “Detectron2,” Facebook Research, 2019.
- [47] S. Qiao, L.-C. Chen, and A. Yuille, “Detectors: Detecting objects with recursive feature pyramid and switchable atrous convolution,” 2020.
- [48] Z. Cai and N. Vasconcelos, “Cascade r-cnn: Delving into high quality object detection,” 2017.
- [49] T.-Y. Lin, P. Dollár, R. Girshick, K. He, B. Hariharan, and S. Belongie, “Feature pyramid networks for object detection,” 2016.
- [50] S. Ioffe and C. Szegedy, “Batch normalization: Accelerating deep network training by reducing internal covariate shift,” 2015.
- [51] X. Chen, “Image enhancement effect on the performance of convolutional neural networks,” 2019.
- [52] A. Kovashka, O. Russakovsky, L. Fei-Fei, and K. Grauman, “Crowdsourcing in computer vision,” *arXiv preprint arXiv:1611.02145*, 2016.
- [53] C. Wah, “Crowdsourcing and its applications in computer vision,” *University of California, San Diego*, 2006.
- [54] P. Welinder and P. Perona, “Online crowdsourcing: rating annotators and obtaining cost-effective labels,” in *Computer Society Conference on Computer Vision and Pattern Recognition-Workshops*. IEEE, 2010.
- [55] R. Di Salvo, D. Giordano, and I. Kavasidis, “A crowdsourcing approach to support video annotation,” in *International Workshop on Video and Image Ground Truth in Computer Vision Applications*, 2013.
- [56] J. Deng, J. Krause, and L. Fei-Fei, “Fine-grained crowdsourcing for fine-grained recognition,” in *IEEE conference on computer vision and pattern recognition*, 2013.
- [57] L. Von Ahn, B. Maurer, C. McMillen, D. Abraham, and M. Blum, “recaptcha: Human-based character recognition via web security measures,” *Science*, vol. 321, no. 5895, pp. 1465–1468, 2008.
- [58] “reCAPTCHA help,” <https://support.google.com/recaptcha/?hl=en>.
- [59] Tramaci, “Anopticon – Mappa delle Telecamere – “Big Brother” Viewer – Il grande fratello (secondo orwell) si sts espandendo.” <http://tramaci.org/anopticon/>.
- [60] OpenStreetMap, “Camera Objects,” <https://wiki.openstreetmap.org/w/index.php?search=camera&title=Special%3ASearch&go=Go>.
- [61] “Gorodskaja sistema videonabljudenija (Moskva) – City video-surveillance system (Moscow),” <https://video.dit.mos.ru/about/>.
- [62] “Carte de l’implantation des caméras de vidéoverbalisation à Paris,” <https://www.data.gouv.fr/fr/reuses/carte-de-limplantation-des-cameras-de-videoverbalisation-a-paris/>.
- [63] “Vidéoprotection - Implantation des caméras,” <https://www.data.gouv.fr/fr/datasets/videoprotection-implantation-des-cameras-kml-ods/>.
- [64] “The spatial distribution of open-street CCTV in the Brussels-Capital Region,” <https://journals.openedition.org/brussels/1427?lang=en>.
- [65] Google, “Publish and connect 360 photos with the Street View app,” <https://support.google.com/maps/answer/7011737?hl=en>, 2018.
- [66] C. Smith, “Travel back in time with Google Street View,” <http://home.bt.com/tech-gadgets/internet/travel-back-in-time-with-google-street-view-11363960715817>, 2018.
- [67] OpenStreetMap, “Routing/online routers,” [https://wiki.openstreetmap.org/wiki/Routing/online\\_routers](https://wiki.openstreetmap.org/wiki/Routing/online_routers).
- [68] —, “Routing/offline routers,” [https://wiki.openstreetmap.org/wiki/Routing/offline\\_routers](https://wiki.openstreetmap.org/wiki/Routing/offline_routers).
- [69] D. Luxen and C. Vetter, “Real-time routing with OpenStreetMap data,” in *Proceedings of the 19th ACM SIGSPATIAL international conference on advances in geographic information systems*, 2011.
- [70] D. Delling, P. Sanders, D. Schultes, and D. Wagner, “Engineering route planning algorithms,” in *Algorithmics of large and complex networks*. Springer, 2009.
- [71] H. Bast, D. Delling, A. Goldberg, M. Müller-Hannemann, T. Pajor, P. Sanders, D. Wagner, and R. F. Werneck, “Route planning in transportation networks,” in *Algorithm engineering*. Springer, 2016.
- [72] R. J. Szczerba, P. Galkowski, I. S. Glicktein, and N. Ternullo, “Robust algorithm for real-time route planning,” *IEEE Transactions on Aerospace and Electronic*

- Systems*, vol. 36, no. 3, pp. 869–878, 2000.
- [73] “Open source routing machine (osrm) – a modern c++ routing engine for shortest paths in road networks.” <http://project-osrm.org/>.
- [74] C. R. Banbury, V. J. Reddi, M. Lam, W. Fu, A. Fazel, J. Holleman, X. Huang, R. Hurtado, D. Kanter, A. Lokhmotov *et al.*, “Benchmarking TinyML Systems: Challenges and Direction,” *arXiv preprint arXiv:2003.04821*, 2020.
- [75] X. Zhang, Y. Wang, and W. Shi, “pcamp: Performance comparison of machine learning packages on the edges,” in *{USENIX} Workshop on Hot Topics in Edge Computing (HotEdge 18)*, 2018.
- [76] A. G. Howard, M. Zhu, B. Chen, D. Kalenichenko, W. Wang, T. Weyand, M. Andreetto, and H. Adam, “Mobilenets: Efficient convolutional neural networks for mobile vision applications,” 2017.
- [77] M. Sandler, A. Howard, M. Zhu, A. Zhmoginov, and L.-C. Chen, “MobileNetV2: Inverted residuals and linear bottlenecks,” in *Proceedings of the IEEE conference on computer vision and pattern recognition*, 2018, pp. 4510–4520.
- [78] I. Kim, “tf-mobilenet-v2 – mobilenet v2 (inverted residual) implementation & trained weights using tensorflow,” <https://github.com/ildoonet/tf-mobilenet-v2>, 2015.
- [79] K. Han, Y. Wang, Q. Tian, J. Guo, C. Xu, and C. Xu, “GhostNet: More features from cheap operations,” in *Proceedings of the IEEE/CVF Conference on Computer Vision and Pattern Recognition*, 2020, pp. 1580–1589.
- [80] H. N. A. Lab”, “Ghostnet implementation using tensorflow/pytorch,” <https://github.com/huawei-noah/ghostnet>, 2020.
- [81] F. Gustafsson, *Statistical sensor fusion*. Studentlitteratur, 2010.
- [82] L. Winkley and T. Figueroa, “San Diego has more than 3,000 cameras on street-lights,” <https://www.sandiegouniontribune.com/news/public-safety/story/2020-03-01/san-diego-has-3-000-cameras-on-street-lights-do-they-target-any> computer vision on google street view,” 2018.
- [83] B. I. Team, “Skripal Suspect Boshirov Identified as GRU Colonel Anatoliy Chepiga,” 2018.
- [84] —, “Full Report: Skripal Poisoning Suspect Dr Alexander Mishkin Hero of Russia,” 2018.
- [85] M. Farrell, “Assassination and Poisoning,” in *Criminology of Poisoning Contexts*. Springer, 2020, pp. 69–92.
- [86] C. Levett, F. Sheehy, P. Guest, and L. Smears, “Visual guide: how the novichok suspects made their way to Salisbury,” <https://www.theguardian.com/uk-news/2018/sep/05/novichok-poisoning-what-we-know-so-far>, 2018.
- [87] M. Guri and D. Bykhovsky, “air-jumper: Covert air-gap exfiltration/infiltration via security cameras & infrared (ir),” *Computers & Security*, vol. 82, pp. 15–29, 2019.
- [88] A. Cui, M. Costello, and S. Stolfo, “When firmware modifications attack: A case study of embedded exploitation,” 2013.
- [89] A. Costin and J. Zaddach, “IoT malware: Comprehensive survey, analysis framework and case studies,” *BlackHat USA*, 2018.
- [90] R. Girshick, I. Radosavovic, G. Gkioxari, P. Dollár, and K. He, “Detectron,” 2018.
- [91] F. Massa and R. Girshick, “Faster R-CNN and Mask R-CNN in PyTorch 1.0,” Facebook Research, Apr. 2020.
- [92] “COCO - Common Objects in Context,” <http://cocodataset.org/#home>.
- [93] M. Everingham, L. V. Gool, C. K. I. Williams, J. Winn, and A. Zisserman, “The PASCAL Visual Object Classes (VOC) challenge,” 2010.
- [94] “The PASCAL Visual Object Classes,” <http://host.robots.ox.ac.uk/pascal/VOC/>.
- [95] M. Everingham and J. Winn, “The PASCAL Visual Object Classes Challenge 2012 (VOC2012) Development Kit,” 2012.
- [96] L. Jiao, F. Zhang, F. Liu, S. Yang, L. Li, Z. Feng, and R. Qu, “A survey of deep learning-based object detection,” *IEEE Access*, vol. 7, 2019. [Online]. Available: <http://dx.doi.org/10.1109/ACCESS.2019.2939201>
- [97] O. Russakovsky, J. Deng, H. Su, J. Krause, S. Satheesh, S. Ma, Z. Huang, A. Karpathy, A. Khosla, M. Bernstein, A. C. Berg, and L. Fei-Fei, “Imagenet large scale visual recognition challenge,” 2014.
- [98] A. Kuznetsova, H. Rom, N. Alldrin, J. Uijlings, I. Krasin, J. Pont-Tuset, S. Kamali, S. Popov, M. Mallocci, A. Kolesnikov, T. Duerig, and V. Ferrari, “The open images dataset v4: Unified image classification, object detection, and visual relationship detection at scale,” *IJCV*, 2020.
- [99] “Open Images Dataset V6 + Extensions,” <https://storage.googleapis.com/openimages/web/index.html>.
- [100] D. Anguelov, C. Dulong, D. Filip, C. Frueh, S. Lafon, R. Lyon, A. Ogale, L. Vincent, and J. Weaver, “Google street view: Capturing the world at street level,” *Computer*, vol. 43, no. 6, pp. 32–38, 2010.
- [101] S. I. L. Paiva, “Inferring urban indicators through computer vision on google street view,” 2018.
- [102] Z. Wojna, A. N. Gorban, D.-S. Lee, K. Murphy, Q. Yu, Y. Li, and J. Ibarz, “Attention-based extraction of structured information from street view imagery,” in *14th IAPR International Conference on Document Analysis and Recognition (ICDAR)*. IEEE, 2017.
- [103] K. Hara, V. Le, and J. Froehlich, “A feasibility study of crowdsourcing and Google Street View to determine sidewalk accessibility,” in *14th international ACM SIGACCESS conference on Computers and accessibility*, 2012.
- [104] —, “Combining crowdsourcing and Google Street View to identify street-level accessibility problems,” in *SIGCHI conference on human factors in computing systems*, 2013.
- [105] K. Hara, J. Sun, R. Moore, D. Jacobs, and J. Froehlich, “Tohme: detecting curb ramps in Google Street View

- using crowdsourcing, computer vision, and machine learning,” in *27th annual ACM symposium on User interface software and technology*, 2014.
- [106] K. Hara, S. Azenkot, M. Campbell, C. L. Bennett, V. Le, S. Pannella, R. Moore, K. Minckler, R. H. Ng, and J. E. Froehlich, “Improving public transit accessibility for blind riders by crowdsourcing bus stop landmark locations with Google Street View: An extended analysis,” *ACM Transactions on Accessible Computing (TACCESS)*, 2015.
- [107] A. R. Zamir and M. Shah, “Accurate image localization based on Google Maps Street View,” in *European Conference on Computer Vision*. Springer, 2010.
- [108] M. Turk and A. Pentland, “Face recognition using eigenfaces,” in *Proceedings of IEEE computer society conference on computer vision and pattern recognition*, 1991.
- [109] V. Bruce and A. Young, “Understanding face recognition,” *British journal of psychology*, vol. 77, no. 3, pp. 305–327, 1986.
- [110] R. Brunelli and T. Poggio, “Face recognition: Features versus templates,” *IEEE transactions on pattern analysis and machine intelligence*, vol. 15, no. 10, pp. 1042–1052, 1993.
- [111] T. Ahonen, A. Hadid, and M. Pietikäinen, “Face recognition with local binary patterns,” in *European conference on computer vision*, 2004.
- [112] A. K. Jain and S. Z. Li, *Handbook of face recognition*, 2011.
- [113] P. J. Phillips, P. J. Flynn, T. Scruggs, K. W. Bowyer, J. Chang, K. Hoffman, J. Marques, J. Min, and W. Worek, “Overview of the face recognition grand challenge,” in *Computer society conference on computer vision and pattern recognition*. IEEE, 2005.
- [114] O. M. Parkhi, A. Vedaldi, and A. Zisserman, “Deep face recognition,” 2015.
- [115] L. J. Halawa, A. Wibowo, and F. Ernawan, “Face Recognition Using Faster R-CNN with Inception-V2 Architecture for CCTV Camera,” in *2019 3rd International Conference on Informatics and Computational Sciences (ICICoS)*, 2019.
- [116] S. Ren, K. He, R. Girshick, and J. Sun, “Faster r-cnn: Towards real-time object detection with region proposal networks,” 2015.
- [117] S. Bah and F. Ming, “An improved face recognition algorithm and its application in attendance management system,” *Array*, vol. 5, 2019.
- [118] M. Mileva and A. Burton, “Face search in cctv surveillance,” *Cognitive research: principles and implications*, vol. 4, no. 3, 2019.
- [119] A. Kofman, “Losing Face How a Facial Recognition Mismatch Can Ruin Your Life,” <https://theintercept.com/2016/10/13/how-a-facial-recognition-mismatch-can-ruin-your-life/>, 2016.
- [120] A. Kaganskih, ““Big Brother” for sale, or the “Black Markets” of a “Safe Smart City”. Video report. (Bol’shoj Brat optom i v roznicu, ili Chernyj rynek “Bezopasnogo goroda”. Videoreportazh.),” <https://mbk.news/suzhet/bolshoj-brat-optom-i-v-roznicu/>, Dec 2019.
- [121] M. Bishop and C. Gates, “Defining the insider threat,” in *4th annual workshop on Cyber security and information intelligence research*, 2008.
- [122] L. Spitzner, “Honeypots: Catching the insider threat,” in *19th Annual Computer Security Applications Conference*. IEEE, 2003.
- [123] A. Cui and S. J. Stolfo, “A quantitative analysis of the insecurity of embedded network devices: results of a wide-area scan,” in *26th Annual Computer Security Applications Conference*, 2010.
- [124] A. Costin, J. Zaddach, A. Francillon, and D. Balzarotti, “A large-scale analysis of the security of embedded firmwares,” in *23rd USENIX Security Symposium*, 2014.
- [125] A. Costin, A. Zarras, and A. Francillon, “Automated dynamic firmware analysis at scale: a case study on embedded web interfaces,” in *11th ACM on Asia Conference on Computer and Communications Security*, 2016.
- [126] C. Heffner, “Exploiting surveillance cameras,” 2013.
- [127] A. Costin, “Poor Man’s Panopticon: Mass CCTV surveillance for the masses,” *PowerOfCommunity*, November, 2013.
- [128] S. Shekyan and A. Harutyunyan, “To Watch Or To Be Watched. Turning your surveillance camera against you,” *HITB AMS*, 2013.
- [129] “Insecam – online cameras directory,” <https://insecam.org>, 2013.
- [130] H. Xu, F. Xu, and B. Chen, “Internet protocol cameras with no password protection: An empirical investigation,” in *International Conference on Passive and Active Network Measurement*, 2018.
- [131] B. Krebs, “Source code for IoT botnet “Mirai” released,” *KrebsonSecurity*.(Oct. 2016). Retrieved Feb, 2016.

#### APPENDIX



Fig. 15: Examples of directed camera class (images CC0 by unsplash.com).





Fig. 16: Examples of round camera class (images CC0 by unsplash.com).



Fig. 17: Example of a hybrid installation consisting of a light pole combined with a CCTV camera. Our TridentNet model works well with a detection confidence of 97% of the “round class” instance, and avoids the potential “directed class” FP represented by the light fixture below the camera.

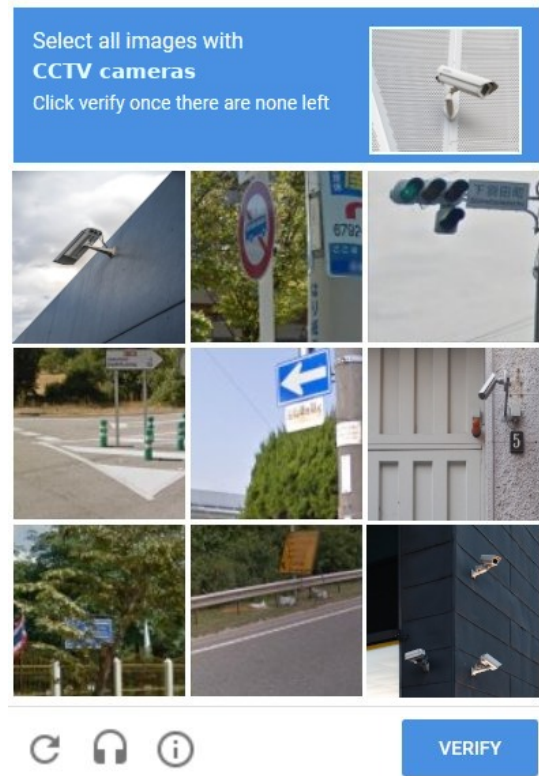


Fig. 19: Our proposed vision for a novel reCAPTCHA V2 extension offering “Select all images with CCTV cameras” to better and faster help annotate and validate the CCTV camera objects in Google Street View imagery.

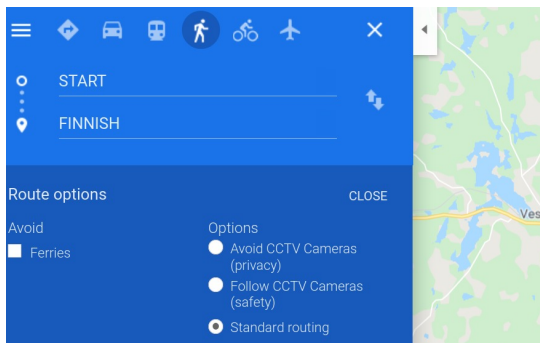


Fig. 18: Our proposed vision for a novel map navigation that provides the users both privacy (“Avoid CCTV Cameras (privacy-first)”) and safety (“Follow CCTV Cameras (safety-first)”) route planning options.

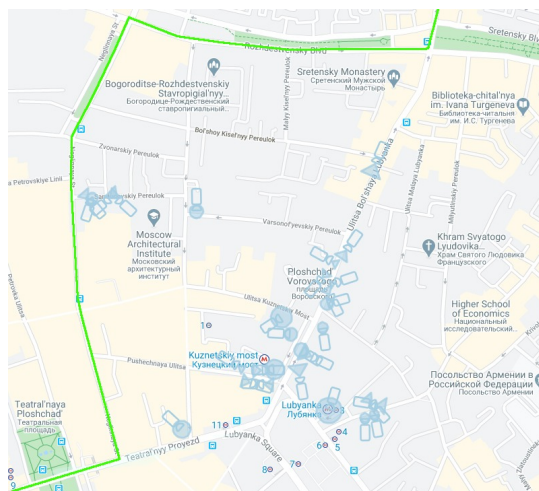


Fig. 20: Google Maps prototype: CCTV-aware routing system providing route for “Avoid CCTV Cameras (privacy-first)” user option.

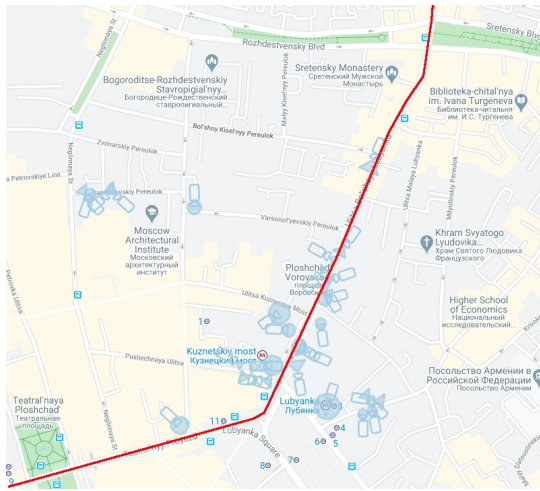


Fig. 21: Google Maps prototype: CCTV-aware routing system providing route for “Follow CCTV Cameras (safety-first)” user option.



Fig. 22: Mobile device prototype in action – camera detected, lasers activated. Top screen shows the RPi4 internal view. Bottom screen shows a CCTV camera instance to test the mobile device.

---

### Algorithm 1 CCTV-aware mobile device operation

---

**Input:** –

**Output:** location and meta data of CCTV cameras

*INIT :*

- 1: START autonomous operation
  - 2: **while** (TRUE) **do**
  - 3:   SCAN with Pan-Tilt HAT with PiCamera street level imagery
  - 4:   **if** (CCTV camera object IS detected) **then**
  - 5:     CENTER with Pan-Tilt HAT both range finder and PiCamera on the detected CCTV camera
  - 6:     **OPTIONAL:** TRIGGER special lasers for camera-blinding (“pro-active privacy” approach)
  - 7:     TRIGGER PiCamera
  - 8:     CAPTURE with PiCamera visual sample for data validation (e.g., reCAPTCHA in Section IV-A1)
  - 9:     TRIGGER laser-based range finder
  - 10:    CAPTURE with range finder accurate distance from the mobile device to the detected CCTV camera
  - 11:    COMBINE range finder distance with accurate GPS location from the GPS dongle
  - 12:    UPDATE/ADD CCTV camera meta-data (visual, exact location) to the global real-time map
  - 13:    SAVE CCTV camera data / SEND to API cloud
  - 14:    **end if**
  - 15: **end while**
  - 16: **return** *CCTV\_DATA*
-



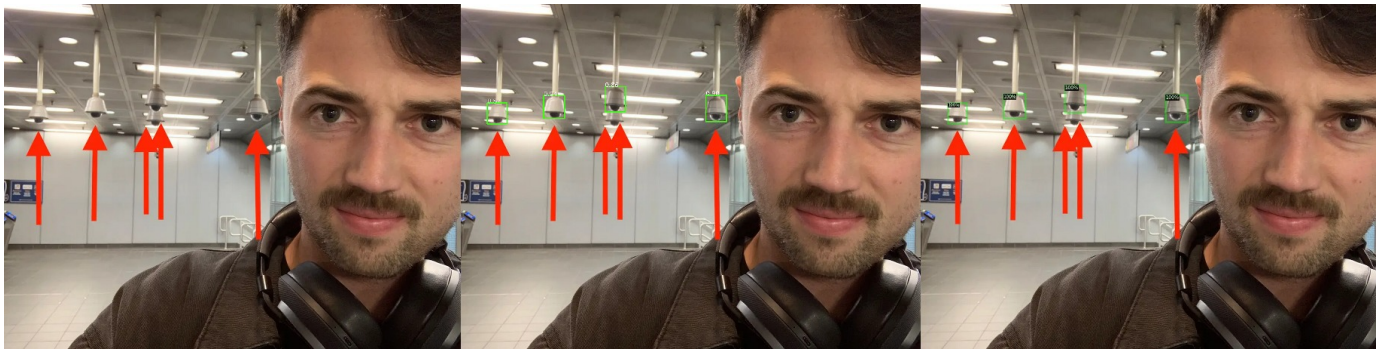


Fig. 23: Visual results (left to right): Original image (Ground Truth) - 5 TP; ATSS X-101 - 4 TP, 1 FN; TridentNet R-101 - 4 TP, 1 FN

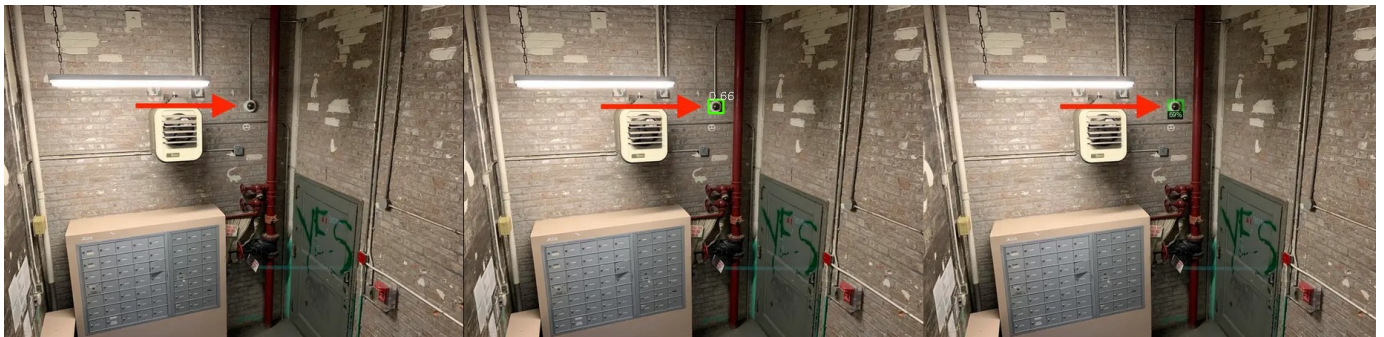


Fig. 24: Visual results (left to right): Original image (Ground Truth) - 1 TP; ATSS X-101 - 1 TP; TridentNet R-101 - 1 TP



Fig. 25: Visual results (left to right): Original image (Ground Truth) - 1 TP; ATSS X-101 - 1 TP; TridentNet R-101 - 1 FN



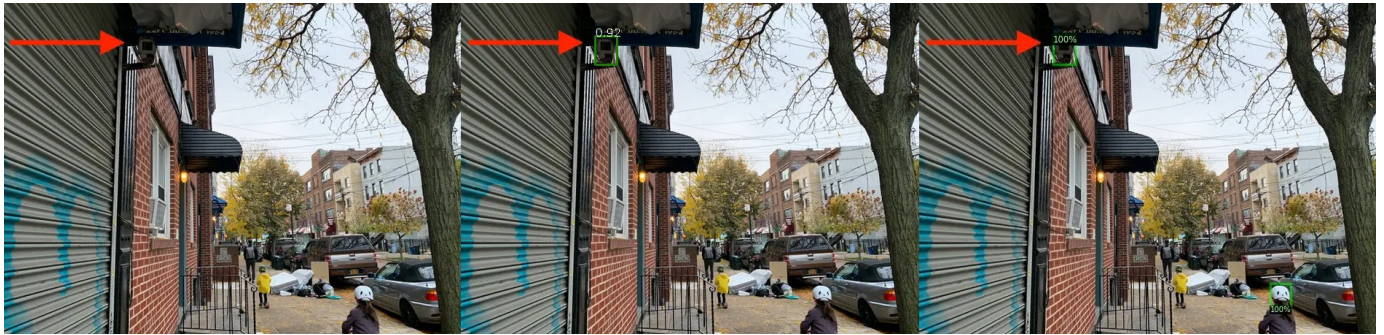


Fig. 26: Visual results (left to right): Original image (Ground Truth) - 1 TP; ATSS X-101 - 1 TP; TridentNet R-101 - 1 TP, 1 FP

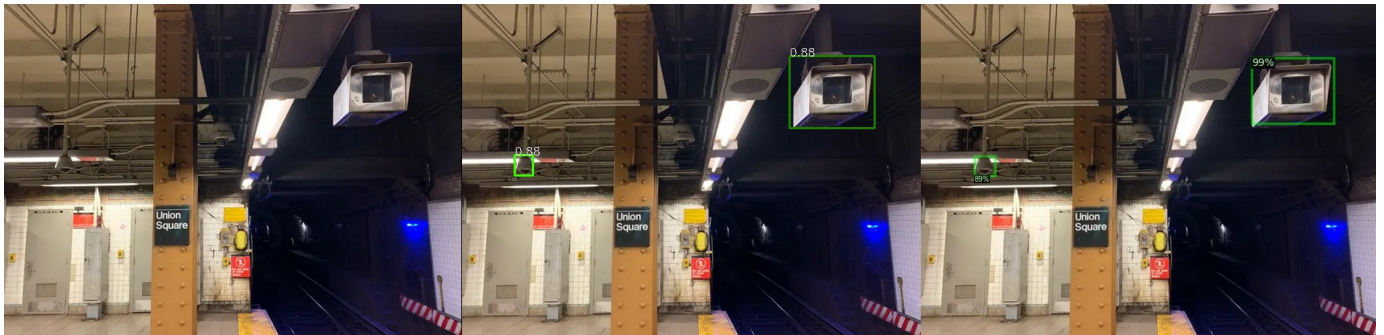


Fig. 27: Visual results (left to right): Original image (Ground Truth) - 2 TP; ATSS X-101 - 2 TP; TridentNet R-101 - 2 TP



Fig. 28: Visual results (left to right): Original image (Ground Truth) - 4 TP; ATSS X-101 - 3 TP, 1 FN; TridentNet R-101 - 3 TP, 1 FN

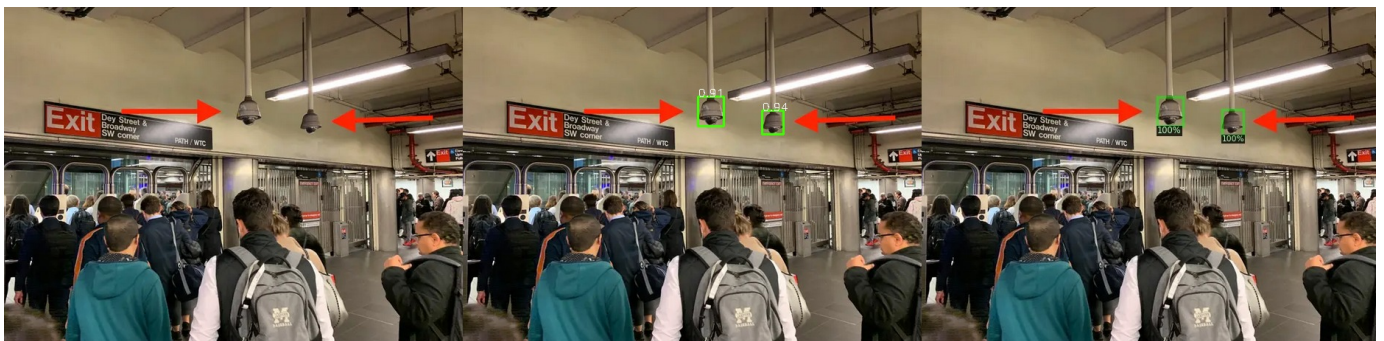


Fig. 29: Visual results (left to right): Original image (Ground Truth) - 2 TP; ATSS X-101 - 2 TP; TridentNet R-101 - 2 TP





**Fig. 30:** Visual results (left to right): Original image (Ground Truth) - 5 TP; ATSS X-101 - 5 TP; TridentNet R-101 - 4 TP, 1 FN



**Fig. 31:** Visual results (left to right): Original image (Ground Truth) - 1 TP; ATSS X-101 - 1 TP; TridentNet R-101 - 1 TP



**Fig. 32:** Visual results (left to right): Original image (Ground Truth) - 1 TP; ATSS X-101 - 1 FN; TridentNet R-101 - 1 TP. NOTE: When the original author's red arrow is removed, it proved quite challenging for humans to quickly detect the CCTV camera as it "hides" behind a corner and blends into the dark background.

**TABLE IX:** Results for bounding box detection with the Dataset0 *testing set* (**bold**=best, underline=worst).

Detector	AP@0.5	AP@0.5:0.95	APs	APm	AR 1	AR 10	ARs	ARm
CM2 Lite V-39	88,2%	63,8%	<b>65,4%</b>	68,7%	61,0%	<b>73,4%</b>	<b>69,7%</b>	78,8%
CM2 V-57	89,7%	62,9%	62,8%	66,3%	61,5%	71,5%	65,7%	79,5%
CM2 V-99	90,1%	64,9%	64,3%	<b>70,2%</b>	61,5%	72,9%	68,1%	<b>79,7%</b>
ATSS R-50	86,5%	58,2%	57,4%	63,9%	56,8%	66,0%	60,7%	73,5%
ATSS X-101	<b>91,1%</b>	<b>65,4%</b>	64,4%	70,1%	<b>61,6%</b>	72,3%	67,2%	79,4%
Trident R-101	88,3%	58,7%	<u>56,0%</u>	65,4%	<u>56,3%</u>	<u>65,8%</u>	<u>58,5%</u>	76,0%

**TABLE X:** Results for bounding box detection with the Dataset0 *validation set* (**bold**=best, underline=worst).

Detector	AP@0.5	AP@0.5:0.95	APs	APm	API	AR 1	AR 10	ARs	ARm	ARI
CM2 Lite V-39	93,9%	69,9%	49,9%	72,1%	77,1%	71,1%	76,5%	54,5%	77,5%	85,6%
CM2 V-57	<b>95,6%</b>	<b>74,5%</b>	<b>57,4%</b>	75,9%	81,1%	<b>74,6%</b>	<b>80,3%</b>	<b>60,5%</b>	81,0%	88,0%
CM2 V-99	95,0%	73,3%	55,5%	74,0%	<b>82,1%</b>	74,0%	79,5%	58,8%	79,4%	<b>89,3%</b>
ATSS R-50	93,2%	71,7%	52,3%	74,4%	77,6%	72,9%	78,2%	55,4%	80,0%	86,3%
ATSS X-101	94,3%	73,1%	54,6%	<b>76,0%</b>	78,0%	74,2%	79,6%	57,8%	<b>81,2%</b>	86,8%
Trident R-101	94,0%	70,3%	52,7%	<u>70,9%</u>	79,8%	73,0%	77,6%	55,6%	78,7%	86,8%

**TABLE XI:** Detector configuration, iterations count, training and inference times when training detectors on Dataset0.

Detector	Best-result iterations (number)	Weights file size (MB)	Avg. train time / iter. (seconds)	Avg. inference time / image (seconds)
CM2 Lite V-39	20000	281.1	<b>0.28</b>	<b>0.061</b>
CM2 V-57	20000	551.4	0.81	0.089
CM2 V-99	30000	776.0	1.22	0.109
ATSS R-50	30000	<b>264.1</b>	0.48	0.064
ATSS X-101	22500	718.7	<u>2.40</u>	0.132
Trident R-101	20000	421.9	1.59	<u>0.169</u>